PROBING THE UNIVERSAL ROLE OF SEC1/MUNC18 PROTEINS BY MUTAGENESIS OF YEAST SEC1

By

KRISTINA KAORI HASHIZUME

A thesis submitted to the Graduate School-New Brunswick

Rutgers, The State University of New Jersey

and

The Graduate School of Biomedical Sciences

University of Medicine and Dentistry of New Jersey

In partial fulfillment of the requirements

For the degree of

Master of Science

Graduate Program in Microbiology and Molecular Genetics

Written under the direction of

Chavela Carr, Ph.D.

And approved by

_____

_____

_____

New Brunswick, New Jersey

May 2008

ABSTRACT OF THE THESIS

Probing the Universal Role of Sec1/Munc18 Proteins

by Mutagenesis of Yeast Sec1

By KRISTINA KAORI HASHIZUME

Thesis Director:

Chavela Carr, Ph.D.

The Sec1/Munc18 (SM) family of proteins is essential for intracellular vesicle trafficking in eukaryotic cells. Sec1, the SM protein at the yeast plasma membrane, is required for membrane fusion leading to secretion and cell growth. Fusion of exocytic vesicles targeted to the plasma membrane occurs in two stages. The vesicle is first tethered to the membrane by a protein complex called the exocyst. Essential membrane-associated proteins known as the soluble *N*-ethylmaleimide-sensitive factor attachment protein receptors (SNAREs) located on both the plasma membrane and the vesicle assemble together to form a stable four-helix bundle called the SNARE complex. In the second step, Sec1 binds to the assembled SNARE complex and there is fusion of the two membranes.

Sec1 has been shown to bind the SNARE complex, but the exact role and mechanism of Sec1 function remains unknown. In this study, site-directed mutagenesis was used to

investigate the significance of highly conserved salt bridges in SM proteins and define the SNARE complex binding surface on Sec1 with data from random mutants studied by Yi-Shan Cheng and Jenna Hutton. In addition, Sec1 mutants with a novel phenotype were generated that may support a role for Sec1 in vesicle tethering.

Acknowledgements

I would like to acknowledge my advisor, Chavela Carr, Ph.D. for her support and insight, Yi-Shan Cheng, for her patience and supervision, and Jenna Hutton, Ph.D. and Adam Weinglass Ph.D. for their direction and guidance.

I am grateful to my committee members Terri Goss Kinzy, Ph.D. and Barth Grant, Ph.D. for their assistance and support.

I would like to thank Rajesh Patel for help with electron microscopy, Joe Kramer, Ph.D., for the leucine mutant, Don Winkleman, Ph.D., for help with Adobe Photoshop, and Vikas Nanda, Ph.D. for his help with structural analysis.

I am especially grateful to my fiancé, Joe, and my family for their love and continuous support.

Table of Contents

List of Tables

List of Figures

I. Introduction

Intracellular membrane fusion is critical for viability. On a cellular level, fusion is required for endocytosis, exocytosis, cell growth and vesicle trafficking. More broadly, it is required for proper functioning of the endocrine system, the release of neurotransmitters from the synapse, and is used by enveloped viruses to enter the cell. The active process leading to the mixing of vesicle and target membranes must not only be efficient, but also specific for cargo as well as target membrane. Deregulation of membrane fusion events results in a variety of genetic diseases including Inclusion-cell disease (Olkkonen and Ikonen, 2000) and Hermansky-Pudlak Syndrome (Suzuki *et al.*, 2003).

The Sec1/Munc18 (SM) family of proteins is essential for vesicle fusion in eukaryotic cells. Although the mechanism of their function is unknown, they have been shown to interact with membrane-associated proteins known as the soluble *N*-ethylmaleimide-sensitive factor attachment protein receptors (SNAREs), anchored on vesicles (v-SNAREs) and target membranes (t-SNAREs). The assembly of SNAREs into a four-helix bundle, or the SNARE complex, is sufficient to fuse liposomes in vitro, but the process is very slow (Weber *et al.*,1998). Addition of the SM protein, Munc18-1, is shown to accelerate and specify this fusion by binding explicitly to its cognate SNARE complexes (Shen *et al.*, 2007).

SM proteins function at different intracellular membrane compartments. Sec1 is critical for fusion of vesicles with the plasma membrane (Novick and Schekman, 1979), Vps33 functions between the endosomes and the vacuole (Banta *et al.*, 1990), Vps45 between the golgi and the vacuole/late endosomes (Cowles *et al.*, 1994) and Sly1 for ER to golgi transport (Ossig *et al.*, 1991). As early work highlighted the specific interactions of SM proteins with their individual SNAREs (Misura *et al.*, 2000, Grabowski and Gallwitz, 1997, Hu *et al.*, 2007, Bracher and Weissenhorn, 2002, Bryant and James 2003, Dulubova *et al.*, 2002, and Shen *et al.*, 2007) the conserved function of SM proteins was unclear. However, recent studies in Vps45 (Carpp *et al.*, 2006), Sly1 (Li *et al.*, 2005) and Munc18-1 (Dulubova *et al.*, 2007) unify the SM proteins under a common and essential role first suggested with Sec1, which binds assembled SNARE complexes (Carr *et al.*, 1999). This conserved function is supported by a unique polypeptide fold common to this family, seen in the crystal structures of Sly1 and Sec1 orthologs. SM proteins are arch-shaped, with ~ 600 amino acids and a molecular weight of 60-90 kDa (Li *et al.*, 2005). The amino acid sequence starts at domain 1 followed by the first half of domain 2, domain 3a, 3b, and then the remainder of domain 2 (Misura *et al.*, 2000). The insertion of the domain 3 sequence within domain 2 leads to a unique "fold-back" in the structure. The conservation of this structure suggests that it may be necessary for the mechanism in which SM proteins function.

Targeting and fusing vesicles at the membrane is highly regulated and requires a large set of proteins, which vary by intracellular compartment and among species (Toonen and Verhage 2003). Generally, a new vesicle is targeted to the membrane through the action

of actin and the cytoskeleton and is secured at a distance (>25nm) from the membrane by tethering proteins (Pfeffer, 1999). A tighter association leads to the docking of the vesicle (<5-10nm), SNARE complex formation and subsequent fusion of the two membranes (Pfeffer, 1999).

In yeast, vesicle fusion at the plasma membrane is mediated by the SM protein, Sec1. Secretory vesicles of two classes (Harsay and Bretscher, 1995) are targeted to active sites of secretion at the bud tip and the bud neck at cytokinesis. These vesicles are tethered to the plasma membrane by a multiprotein complex known as the exocyst (Terbush *et al.*, 1996, Guo *et al.,* 1999). The exocyst is assembled from subunits on the vesicle and the plasma membrane and is important for the targeting and tethering of secretory vesicles to sites of exocytosis (Boyd *et al.,* 2004). Sec1 is concentrated at exocytic sites and has been shown to bind to the exocytic SNARE complex (Carr *et al.,* 1999). In yeast, the exocytic SNARE complex consists of the v-SNARE, Snc, and the plasma membrane t-SNAREs, Sso and Sec9. Sec1 binding to the SNARE complex suggests a role for after SNARE complex assembly (Grote *et al.*, 2000), in docking and fusion. In addition, recent evidence suggests a possible interaction with the exocyst during tethering (Wiederkehr *et al.*, 2004), but the exact role(s) of Sec1 in vesicle docking and fusion remains unclear.

Evidence from X-ray crystal structures may support ligand-induced conformational change as a possible mechanism for SM protein function. The comparison of three crystal structures of squid neuronal Sec1 (sSec1) and rat neuronal Sec1 (nSec1) (Bracher

and Weissenhorn, 2001) has been found to result in a ligand-induced rotational movement of domain 1. While the structure of nSec1 bound to the monomeric neuronal t-SNARE, syntaxin1a, has a cavity of 23 Å, the central cavity of the uncomplexed sSec1 is 10 Å wider (Bracher *et al.*, 2000). In addition, limited contact between domain 3a and the rest of nSec1 support a possible hinge location for outward movement of the domain (Misura *et al.*, 2000).

To better understand the interaction between Sec1 and the SNARE complex, we generated mutants to identify regions of Sec1 necessary for the conserved function of SNARE complex binding. Use of *Saccharomyces cerevisiae* as a model organism allowed us to exploit the conditionality of temperature sensitive mutants to study the otherwise lethal mutations of the essential gene. Through site-directed mutagenesis of residues conserved across the SM family and analysis of directed and random mutants, we were able to map the SNARE complex binding surface on Sec1 and isolate mutants with a novel Sec1 phenotype. These results support a dual role for Sec1 in both vesicle tethering and membrane fusion.

II. Importance of highly conserved residues in SM proteins

2.1 Conserved residues are shared across the SM family

The four families of SM proteins mediate fusion at different steps in exocytosis. Although they have diverged to work at specific compartments and at different stages of trafficking, their unique structure has been conserved at each step and across broad evolutionary distances (Hutton *et al.*, in review). The conservation of this protein for a critical function suggests evolutionarily conserved sites in the amino acid sequence. Previous work in comparative genomics identified shared conserved sites across the SM proteins and also specific sites conserved within each family (Hutton *et al.*, in review). While some conserved sites map to domain 3a, the majority of conserved sites are packed together and buried in domain 2 (Figure 1A).

In order to understand the significance of these conserved sites, we analyzed residues that were over 90% conserved by amino acid identity. Interestingly, half of these residues were involved in two salt bridges, buried in domains 2 and 3a (Figure 1A). From studies in other protein families, it has been shown that the majority of salt bridges are not conserved for all members of that family (Schueler and Margalit, 1995). By contrast, SM proteins share two salt bridges conserved in all four members over broad evolutionary divergence (Hutton *et al.*, in review) suggesting a significant role for these salt bridges. In order to investigate this possibility, site-directed mutagenesis was used to design mutations to substitute the residues of the conserved salt bridges.

2.2 Two salt bridges are conserved in SM proteins

While buried charges destabilize proteins, the formation of a salt bridge can neutralize the charge to stabilize protein structures (Barlow and Thornton, 1983). Salt bridges form between pairs of oppositely charged residues (Asp, or Glu with Arg, Lys, or His) within a distance of 4Å (Kumar and Nussinov, 1999). Although salt bridges can compensate for destabilizing buried charges, hydrophobic residues tightly pack together for increased stabilization and are more commonly found in the core of globular proteins (Hendsch and Tidor, 1994).

Two salt bridges conserved in the SM family are R252-E604 and D307-H371 in domains 2 and 3a, respectively. The location of the R252-E604 buried salt bridge at the core of the protein is intriguing in that buried salt bridges destabilize proteins compared to hydrophobic interactions (Schueler and Margalit, 1995). While the remainder of the Sec1 core is made up of many hydrophobic residues, the preservation of the R252-E604 salt bridge is puzzling.

2.3 Analysis of the salt bridge conserved in domain 3a

In domain 3a of nSec1, residue D307 forms a conserved salt bridge with H371, connecting the two alpha helices that extend the domain. As most salt bridges are responsible for stabilizing tertiary structure (Barlow and Thornton 1983), this salt bridge

may serve a purely structural purpose. To test this, mutant Sec1[D307H,H371D] was designed with reversed charges of the salt bridge. Despite the fact that the microenvironment around the residues can affect salt bridge stability (Schueler and Margalit, 1995), the reversal of the salt bridge did not demonstrate a temperature sensitive growth defect (Figure 2A). This could be explained by the ability of the structure to compensate for the changes due to the relatively isolated position of the domain (Misura *et al*., 2000).

In a second attempt, mutants were designed to destroy the salt bridge by introducing like-charged single amino acid substitutions. Two single mutants, Sec1[D307H] and Sec1[H371D], were designed to have either two positively charged residues or two negatively charged residues in the place of the conserved salt bridge. These mutants were expected to destabilize the domain, but were surprisingly neither were temperature sensitive (Figure 2A).

Why, then, is the D307-H371 salt bridge in domain 3a conserved? Although the reason is unclear, there is some evidence supporting the significance of these residues in a sensitized background (see Appendix 2). In addition, variation in the alignments and the absence of a yeast Sec1 structure could have led to the mutation of an aspartic acid and histidine that did not map to the same location as seen in the nSec1 structure. For these reasons, although the salt bridge is highly conserved across the SM protein family, the mutants designed here were not able to uncover the significance of this conservation.

2.4 Domain 2 salt bridge may be conserved for the flexibility of Sec1

Another highly conserved salt bridge can be found buried in domain 2 located at the center core of the protein. The arginine at position 252 and the glutamic acid at 604 are 100% conserved in the alignment of SM proteins (Hutton *et al.*, in review). As the two residues are located on opposite sides of domain 3 in the primary amino acid sequence, they may be important for stabilizing the unique "fold-back" structure of SM proteins (Figure 1A).

In order to test the significance of the R252-E604 salt bridge, it was replaced with a reversed salt bridge. By reversing the charges at both positions, the Sec1[R252E, E604R] mutant would be expected to maintain the conserved protein structure and exhibit no temperature sensitive growth defect. Surprisingly, reversing the charges in this salt bridge was lethal. One possible explanation for this outcome could be that the chemistry of the surrounding residues was incompatible with the new locations of the charged residues. Compared with D307-H371, the location of R252-E604 is more buried in the interior of the protein as opposed to the isolated domain 3a. The proximity of the tightly packed surrounding residues may have conflicted with the charges leading to the lethal phenotype.

In addition to hydrophobic residues at the protein core, SM proteins have a potentially destabilizing salt bridge. The conservation of such a core may indicate an exclusive function for salt bridges necessary at that position, which cannot be replaced by

hydrophobic residues. To test this, a double leucine mutant, Sec1[R252L,E604L], was designed to keep the long aliphatic side chain, but without the charge of arginine and glutamic acid. The hydrophobic residues were not able to replace the role of the conserved salt bridge leading to a temperature sensitive growth defect. The protein was demonstrated to be stable, ruling out the trivial possibility of conflicting surrounding residues that may have led to destabilization (Figure 3A). This suggests that this salt bridge may not be simply for structural stability, but for another purpose that cannot be substituted by hydrophobic leucines.

To better understand the significance of this conserved salt bridge, single alanine substitutions were designed to break the ionic bond. The small size of alanine may be less likely than the longer leucine side chain to pose a conflict with surrounding residues. If this conserved salt bridge was serving a functional purpose, replacing R252 or E604 individually with alanine mutations was expected to exhibit a temperature sensitive growth defect. While Sec1[E604A] was temperature sensitive as expected, it was interesting to see that Sec1[R252A] was not (Figure 2A). Was the integrity of this conserved salt bridge not necessary?

As a final test, mutants were designed to replace both residues of the salt bridge with alanines. From the degree of conservation of these residues and the temperature sensitivity of Sec1[R252L,E604L], it was expected that replacing the salt bridge with alanines would result in a temperature sensitive growth defect or even lethality. In addition to removing the salt bridge, alanine side chains are unlikely to pack closely to

support a hydrophobic core. A double alanine mutant, Sec1[R252A,E604A] was designed and tested for viability. Surprisingly, this mutant showed no temperature sensitive growth defect despite the lack of the salt bridge (Figure 2B). So, why is this salt bridge so highly conserved?

The inability to replace the salt bridge with hydrophobic residues could indicate that tight packing of the protein core is disadvantageous to Sec1. In support of this, increasing flexibility in the core by replacing the arginine with an alanine residue, as in Sec1[R252A], was not temperature sensitive. Although Sec1[E604A] exhibited a temperature sensitive growth defect, this could be explained by the unpaired charges left buried in the protein. The unpaired arginine of Sec1[E604A] can not be neutralized by deprotonation due to its high pKa of 12. In contrast, the unpaired glutamic acid in Sec1[R252A] with a pKa of 4, can be protonated and neutralized at physiological pH. Removing the salt bridge in Sec1[R252A,E604A] may have introduced more flexibility in the protein core which could explain the viability of this mutant.

Because flexibility may be important for the mechanism of SM protein function, we propose that mutants believed to restrict movement would be too inflexible for SM protein function. Although the exact role of SM proteins remains unclear, the ability to bind SNARE complexes has been conserved for the protein family (Togneri *et al.*, 2006, Carr *et al.*, 1999, Carpp *et al.*, 2006, Shen *et al.*, 2007, Hu *et al.*, 2007, Dulubova *et al.*, 2007, Li *et al.*, 2005). To test if flexibility is important for SNARE complex binding, Sec1[R252A,E604A] and Sec1[R252L,E604L] were tested for their interaction with the

exocytic SNARE complex by using a Sec1 IP protocol followed by immunoblot detection for Sso1. Sso1 can be used as a reporter for the assembled SNARE complex as, in yeast, Sec1 binds exclusively to the ternary complex consisting of t-SNAREs, Sso1 and Sec9 and the v-SNARE, Snc (Togneri *et al.,* 2006). Although Sec1[R252L,E604L] binds the SNARE complex at 25°C, it shows diminished binding after 20 minutes at 38°C, when hydrophobic interactions are increased (Figure 4A). On the other hand, Sec1[R252A,E604A] shows no defect in binding to SNARE complexes, possibly indicating that Sec1 flexibility is important for function (Figure 4A).

A model that proposes a requirement for movement in the protein could explain the high conservation of the R252-E604 salt bridge amid a hydrophobic core. As demonstrated, a mutant with a rigid hydrophobic core was deficient in function compared to wild type or other mutants with more flexible protein cores. Taken together, these results suggest a requirement for flexibility in the region of the R252-E604 salt bridge, a notion supported by differences in crystal structures between complexed and uncomplexed neuronal Sec1 orthologs (Bracher *et al.*, 2000).

2.5 Significance of D255

Another highly conserved residue isolated from the alignment of the SM superfamily is an aspartic acid at position 255. Although aspartic acid has an acidic side chain, it is the backbone carbonyl that binds the R252 side chain, forming a hydrogen bond (Figure 1B). Due to the nature of the interaction with R252, we expected alanine to substitute well for

aspartic acid. An alanine mutation would lack the charged side chain but still be able to maintain the hydrogen bond to R252. Although we expected an alanine substitution to be tolerated by the protein, surprisingly, Sec1[D255A] exhibited a temperature sensitive growth defect (Figure 5A).

What was the role of this conserved aspartic acid? To investigate other possibilities, we looked to the crystal structure of nSec1 and found that D255 was located at the beginning of a short alpha helix. In globular proteins, it has been found that interactions between specific side chains at the ends of short alpha helices are important for their stabilization (Zhou *et al.*, 1994). While bonding between the amide hydrogen and the carbonyl oxygen of a residue in a subsequent turn stabilizes the secondary structure of an alpha helix, the lack of intra-helical bonds at the ends requires bonding to boundary residues (Aurora and Rose, 1998). These boundary residues "cap" the N-terminal (N-cap) or C-terminal (C-cap) ends by fulfilling the hydrogen bonds through their polar side chains, stabilizing the ends of the alpha helix (Zhou *et al.*, 1994), also seen in D255 (Figure 1C). The temperature sensitive growth defect seen in Sec1[D255A] may have been due to the inability of the alanine side chain lacking polar groups to contribute as an N-cap.

In order to test if the aspartic acid at position 255 was important for helix capping, it was substituted with asparagine, the most preferred N-cap residue (Doig and Baldwin, 1995). Asparagine was an ideal candidate for substitution, as it is isosteric to aspartic acid but is neutral in charge. Although the restoration of the N-cap resulted in viability at 38ºC, Sec1[D255N] still exhibited a slightly temperature sensitive growth defect (Figure 5A).

This may suggest that, although it is fulfilling the role as an N-cap, D255 may be conserved for another purpose.

To understand the significance of this position, the genomes of other species were searched to see which other amino acids were suitable for substitution. Although D255 is highly conserved at 99% amino acid identity among 179 SM protein sequences, (Hutton *et al.*, in review), in two sequences it was found to be a glutamic acid residue. Interestingly, glutamic acid is a relatively poor N-cap (Doig and Baldwin, 1995).

One possible explanation for the necessity of an acidic residue at position 255 could be to serve as a salt bridge intermediate during protein folding. The close proximity of D255 to the conserved R252-E604 salt bridge could indicate a possible association between the two. In addition, to conserve the unique fold-back structure of SM proteins, R252 in domain 2 must remain unpaired during the folding of domain 3a and 3b in order to form the final salt bridge with E604. D255 may temporarily salt bridge with R252 as a folding intermediate before being replaced by E604 to form the final conformation as observed in the crystal structures. On the other hand, the stability of Sec1[D255A] at both 25°C and 38°C (Figure 3A), suggests that the protein is capable of folding without this residue, pointing to another role for D255.

In a similar mode of interaction, D255 may be important to form a salt bridge with R252 in a different conformation of Sec1 not seen in the resolved crystal structures. Salt bridge rearrangements have been captured in crystal structures during ligand-induced

conformational change (Jeffrey *et al.*, 1998). By sampling the tolerated rotamers of D255 without altering the backbone configuration, it was determined that an R252-D255 salt bridge can be sterically accommodated within the constraints of salt bridge distance of 4Å (Barlow and Thornton, 1983).

Evidence for conformational change in nSec1 orthologs supports the possibility for movement in SM proteins (Bracher and Weissenhorn, 2002). While this binding mode is specific to some SM proteins, a similar change may occur in the conserved binding of SM proteins to the SNARE complex. In order to support this model, identification of conformational changes can be assayed by comparing protein fragments from limited proteolysis (Rajavel *et al.*, 1996, Fontana *et al.,* 2004, and Carr *et al.*, 1997). If limited flexibility in Sec1[R252L,E604L] resulted in constricted movement of Sec1, we expect that the protein would be less accessible to protease, resulting in fewer digestion fragments compared to wild type. In comparison, proteolysis of the Sec1[R252A,E604A] is expected to yield greater or equal number of fragments compared to wild type, due to its increased flexibility. These mutants were made in the high expression vector, pYES/CT, and frozen for future purification and limited proteolysis experiments, which may provide evidence for conformational differences in SM proteins.

While hydrophobic interactions are highly conserved to stabilize the core of globular proteins, the role of conserved salt bridges is protein specific (Schueler and Margalit 1999). Salt bridges have been conserved for their functional importance in ligand binding sites (Koenderink *et al.*, 2004 and Stockner *et al.*, 2005) stabilizing folding

intermediates (Tissot *et al.*, 1996 and Schueler and Margalit, 1995) and have been demonstrated to rearrange during conformational change (Jeffrey *et al.*, 1998). In the analysis of five conserved residues, two major salt bridges have been found to be conserved across the SM family of proteins. While the significance of the D307-H371 salt bridge remains unclear, the R252-E604 salt bridge may be important for maintaining flexibility at the protein core. The conservation of the acidic residue at 255 may be important for a temporary salt bridge during a conformational change essential for SM protein function.

III. Classifying Sec1 mutants

Sec1 was first identified in *Saccharomyces cerevisiae* as part of a screen for temperature sensitive mutants of the yeast secretory pathway and in *Caenorhabditis elegans* as unc18 in a screen for uncoordinated growth (Novick and Schekman, 1979 and Brenner, 1974). The well-characterized mutant, *sec1-1*, displays a temperature sensitive block in secretion and cell-surface growth exhibited by a defect in invertase secretion and an accumulation of vesicles as observed by electron microscopy (Novick and Schekman, 1979). Early work in *sec1-1* was found to have no defect in SNARE complex assembly at early time points (10 minutes, Grote *et al*., 2000). However, after a 20 minute shift to restrictive temperature, the level of total SNARE complexes is seen to diminish in *sec1-1,* thought to be an indirect effect of a block in SNARE recycling (Grote *et al.,* 2000). While Sec1 binds SNARE complexes and is concentrated at sites of secretion (Carr *et al.*, 1999), the exact function of Sec1 in vesicle fusion is unknown. Characterization of new mutants may uncover novel phenotypes for a better understanding of Sec1 and how it functions at the plasma membrane.

3.1 Sec1[E604A] demonstrates a partial secretion block

Sec1[E604A] is a conserved-site mutant isolated in this study to better understand the role of Sec1. In order to characterize Sec1[E604A], it was tested for its binding affinity to the SNARE complex by using a Sec1 IP protocol followed by immunoblot detection of Sso1, a reporter for the SNARE complex. In order to assay for the abundance of

assembled SNARE complexes, a Sec9 IP was performed followed by immunoblot detection of Sso1. Sec1[E604A] showed a decreased abundance of Sec1-bound SNARE complexes (Figure 6A), a phenotype also seen for *sec1-1*. However, unlike *sec1-1*, Sec1[E604A] was found to have wild type levels of SNARE complexes (Sec9 IP,Figure 6A).

New evidence from mutants such a Sec1[E604A] demonstrating wild type levels of SNARE complexes after 20 minutes (Sec9 IP at 38°C, Figure 6A), support the notion that less abundant SNARE complexes are not seen for all Sec1 mutants, possibly indicating a role for Sec1 upstream of SNARE complex assembly.

Cells secrete invertase through the exocytic pathway to break down disaccharides in the medium into usable monosaccharides. Levels of secreted invertase can be used to assay for defects in secretion as vesicles carrying the cargo are blocked from fusion with the plasma membrane and remain internalized in the cell. De-repression of the invertase gene by shifting to low glucose medium stimulates invertase production. *Sec1-1* has been demonstrated to have a block in invertase secretion to accumulate eight times as much internal invertase (Novick and Schekman, 1979). In order to test if Sec1[E604A] has a similar block, cells were shifted into low glucose medium and assayed for internal and total levels of the invertase enzyme. Surprisingly, novel to Sec1 mutants, Sec1[E604A] exhibits no block in invertase secretion (Figure 6B).

To better understand the unusual phenotype of Sec1[E604A], electron microscopy (EM) was used to looked for a visual block in secretion. Wild type yeast constitutively fuse vesicles at the plasma membrane (Walworth and Novick, 1987) leading to very few or no vesicle accumulation (Figure 6A,B). *Sec1-1* has been shown to accumulate 100nm exocytic vesicles at the bud tip as a result of the block in vesicle fusion at the plasma membrane at restrictive temperature (Novick and Schekman, 1979). Interestingly, despite the lack of an invertase secretion defect, electron micrographs of Sec1[E604A] showed vesicles accumulating at 25°C and even more dramatically at 38°C (Figure 6C,D). This result could indicate that Sec1[E604A] was preferentially blocking the secretion of one type of vesicle, while allowing fusion of other invertase-containing vesicles.

The two classes of secretory vesicles that accumulate in late exocytic mutants can be separated into two populations (Harsay and Bretscher, 1995). The major class carries plasma membrane and cell wall components such as Bgl2 proteins (Harsay and Bretscher, 1995). The second class of exocytic vesicles carries periplasmic enzymes such as invertase, destined for secretion through the endosomal compartments (Harsay and Bretscher,1995). The accumulation of two different vesicle classes could indicate two possible pathways for vesicle trafficking that may be specifically regulated by distinct mechanisms.

Preferential block of an exocytic pathway has also been seen in mutants of Exo70 and Cdc42, which are defective in fusion of Bgl2-containing vesicles, but not invertase-

containing vesicles (Adamo *et al.*, 2001 and He *et al.*, 2007). Exo70 marks exocytic sites along the plasma membrane for tethering by the exocyst, and Cdc42 is a Rho GTPase thought to polarize the actin skeleton and regulate docking and fusion machinery (Adamo *et al.*, 2001 and He *et al.*, 2007).

While *sec1-1* and Sec1[E604A] reveal accumulation of polarized vesicles by EM, they differ in their other phenotypes. S*ec1-1* has a block in invertase secretion (Novick and Schekman, 1979) and fewer assembled SNARE complexes at 20 minutes compared to wild type (Grote *et al.*, 2000). Novel mutant alleles from this study, however, show no defect in invertase secretion and demonstrate wild type levels of assembled SNARE complexes.

3.2 Three classes of Sec1 mutants

The varying phenotypes support the division of Sec1 mutants into three classes (Figure 8). Class "A" mutants demonstrate low abundance of assembled SNARE complexes which may lead to the fewer Sec1-bound SNARE complexes as seen by IP and cluster in domain 2b (Figure 8). These mutants accumulate vesicles by EM and exhibit defects in invertase secretion. Class "B" mutants have wild type levels of SNARE complexes assembled, but demonstrate fewer Sec1-bound SNARE complexes indicating a binding defect. These mutants secrete invertase but accumulate polarized vesicles by EM and cluster in domain 2. Lastly, Class "C" is designated for mutants with a temperature sensitive growth defect, but no discernable phenotype in the limits used in the above

mentioned assays. These mutants may be defective at later time points or in a novel function not yet understood for Sec1.

3.3 Sec1 may play a role in vesicle tethering

The different phenotypes support a two-step function for Sec1 at the plasma membrane. In the first step, Sec1 may directly interact with the exocyst (Wiederkehr *et al.*, 2004) leading to, or stabilizing, the assembly of SNARE complexes. In the second step, Sec1 binds the assembled SNARE complexes (Carr *et al.*, 1999) in order to stimulate fusion between the vesicle and target membrane.

The binding of Sec1 to the assembled SNARE complex implicates Sec1 in the docking and fusion step of exocytosis. While SNARE complexes are sufficient for self-assembly and fusion in liposomes (Weber *et al.*, 1998), the addition of the Sec1 ortholog, Munc18-1, has been shown to specify and accelerate this fusion (Shen *et al.*, 2007). Sec1 has been demonstrated to be important for fusion, but does it also play a role before SNARE complex assembly, in vesicle tethering?

Recent studies have shown that the overexpression of Sec1 leads to higher levels of SNARE complexes compared to wild type, and that a fraction of Sec1 coprecipitates with the exocyst (Wiederkehr 2004). Studies of random mutants by Yi-Shan Cheng and Jenna Hutton and directed mutants from this study further support the role for Sec1 in tethering and SNARE complex assembly. Class A mutants demonstrate a SNARE complex

assembly defect that is not seen in the other classes of Sec1 mutants. Furthermore, these mutations cluster to a region of Sec1 that may be responsible for the interaction leading to this phenotype.

3.4 Model for the specific fusion of vesicle classes by Sec1

The fusion of the two classes of vesicles is hypothesized to have different mechanisms of regulation by Sec1. Bgl2-containing vesicles carry components for membrane growth and may be specifically targeted to the bud tip to avoid cell membrane growth at nonspecific locations. To regulate the fusion of these vesicles, Sec1 may need a specific interaction with an exocyst subunit at the plasma membrane. Indeed, there are two subunits, Exo70 and Sec3, which localize to the bud tip independently of the other exocyst subunits, and demarcate exocytic sites (Boyd *et al.*, 2004). In support of this, mutants of Exo70 have the same secretion defect as seen in Class B mutants where invertase is secreted, yet there is vesicle accumulation by EM (He *et al.*, 2007).

In comparison, the fusion of invertase-containing vesicles may not have to be as specific because the proteins are destined for secretion into the medium. Class B mutants are not defective in assembling SNARE complexes, and as Sso1 (Scott *et al.*, 2004), Sec9 (Brennwald *et al.*, 1994), and patches of Sec1 (Scott *et al.,* 2004) are localized throughout the plasma membrane, it is possible that these vesicles can fuse nonspecifically leading to the invertase secretion phenotype. Furthermore, SNAREs and the Sec1 ortholog, Munc18-1, have been demonstrated to be sufficient for fusion (Shen *et al.*, 2007),

supporting the possibility of nonspecific fusion events along the plasma membrane. Class A mutants, however, are defective in assembling SNARE complexes, and although invertase vesicles may be accumulating, they cannot fuse without SNARE complexes and therefore this may explain the invertase defect seen in this class.

In order to test this hypothesis, future experiments include an assay for Blg2 secretion in Class A and B mutants. While a secretory block is seen by EM in Class B mutants, the absence of an invertase secretion defect may indicate a cargo-specific block of the Bgl2-containing vesicles. Mutants of Exo70 and Cdc42 which lack an invertase secretion defect were demonstrated to be deficient in Bgl2 secretion (He *et al.*, 2007 and Adamo *et al.* 2001). This would support the similarity of Class B mutants and Exo70 mutants and may provide evidence for the ability of Sec1 to specifically regulate vesicle fusion.

Current studies by Yi-Shan Cheng may uncover an interaction between Sec1 and the exocyst. The assembly of the exocyst protein complex is required before SNARE complex can assemble (Pfeffer, 1999). Overexpression of wild type Sec1 has been shown to suppress the phenotypes of the exocyst subunits, *sec5*Δ and *exo70*Δ (Wiederkehr *et al.*, 2004). Random and directed mutants of Class A will be overexpressed in exocyst null strains to look for the inability to suppress this phenotype. This could possibly indicate an interaction between Sec1 and the exocyst which may be able to explain the SNARE complex assembly defect seen in Class A mutants.

IV. Defining the SNARE complex binding surface on Sec1

The specific interactions seen between SM proteins and individual SNAREs (Misura *et al.*, 2000, Grabowski and Gallwitz, 1997, Hu *et al.*, 2007, Bracher and Weissenhorn, 2002, Bryant and James 2003, Dulubova *et al.*, 2002, and Shen *et al.*, 2007) make understanding the essential function of SM proteins difficult. As SM proteins are highly conserved, the essential function is expected to be shared across the family of proteins. Recent studies provide evidence that the SNARE complex binding mode first seen in Sec1 (Togneri *et al.*, 2006, Carr *et al.*, 1999) may be the conserved binding mode that is essential in SM proteins. Studies in Vps45 (Carpp *et al.*, 2006), Munc18-1 (Shen *et al.*, 2007, Hu *et al.*, 2007, Dulubova *et al.*, 2007) and Sly1 (Li *et al.*, 2005) support the possibility that the SNARE complex binding mode is the universal binding mode. The general mechanism of SNARE complex binding required for vesicle fusion suggests a shared binding surface that we expect to be conserved in SM proteins for binding to the SNARE complex.

In order to define the SNARE complex binding surface on Sec1, site-directed mutagenesis was used to design mutants based on three approaches. First, the electrostatic surface potentials of nSec1 and yeast Sec1 were compared to that of the neuronal SNARE complex and the yeast SNARE complex, respectively. Second, shape complementarity of surfaces conserved in SM proteins were used to exclude sites based on size dimensions of the SNARE complex. The third approach relied on previous binding studies on mutants generated by random PCR mutagenesis of the Sec1 coding

sequence started by Barbara Siminovich-Blok and Rachel Schecter and developed by Jenna Hutton, Ph.D. and assayed by Yi-Shan Cheng. Based on the results of the screen of random mutants and the mutants generated by site-directed mutagenesis, we favor a SNARE complex binding surface that includes the groove in domain 2 of Sec1. Because the binding of SM proteins to their cognate SNARE complexes is conserved over broad evolutionary distances (Hutton *et al.,* in review), we believe that the results of our efforts to map the SNARE complex binding surface on yeast Sec1 will represent a general mechanism for SNARE complex interaction by SM proteins.

4.1 Charged regions in Sec1 are candidates for mutagenesis

In an attempt to disrupt functionally important contact sites between Sec1 and the SNARE complex, charge repulsion mutations were made to occlude the ligand from a potential binding site. As protein-protein interactions usually occur over a surface area of solvent exposed residues, and in an effort to minimize structural disturbances, only surface exposed residues were considered for mutagenesis.

Although the structures of SM proteins and assembled SNARE complexes are conserved, amino acid sequences are divergent with only few conserved residues buried in the structures (Hutton *et al.*, in review, Fasshauer *et al.*, 1998). Interestingly, the electrostatic surface potentials of the resolved SNARE complexes are strikingly similar: the core of the four-helix bundle is acidic and the terminal ends are basic (Strop *et al.*, 2007). Surface potentials for the SM proteins are not as ordered. While nSec1 shows regions of

positive and negative charge (Misura *et al*., 2000), squid neuronal Sec1 (sSec1) has a larger acidic surface at the center of the protein (Bracher *et al*., 2000). Since the structure of yeast Sec1 is not yet available, charged residues in yeast Sec1 were mapped onto the structure of nSec1 using sequence homology to isolate surface exposed charged patches (Figure 9A).

4.2 Shape complementarity defines three possible binding surfaces

SNARE complex binding surfaces are expected to be conserved among all SM proteins and are expected to be large enough to physically accommodate the dimensions of the SNARE complex. By using the structures of nSec1 and its cognate neuronal SNARE complex as a reference, three possible binding surfaces were identified (Figure 10A). These surfaces collectively form a network of channels that create a "Y" shape in the structures of SM proteins. Each branch of the "Y", a possible binding surface, will be referred to as the "furrow", "cleft" and "groove" (Figure 10A).

The neuronal SNARE complex is a thin and long helical bundle, 15-20Å wide and 120 Å long (Sutton *et al.*, 1998) (Figure 10B). NSec1, on the other hand, is globular with dimensions of 70Å by 85 Å (Misura *et al.,* 2000). The depth of the narrowest binding surface, the groove, is 15Å (Misura *et al.,* 2000, Figure 10B), confirming that part or even most of the SNARE complex may be accommodated in any of the three surfaces. In addition, the dimensions of these three potential binding surfaces are conserved in the structures of Sly1 (Bracher and Weissenhorn 2002), Munc18c (Hu *et al.,* 2007) and squid

neuronal Sec1 (sSec1, Bracher and Weissenhorn 2001, Bracher *et al.,* 2000), supporting a conserved role for the furrow, cleft and groove.

4.3 The furrow mutant binds SNARE complexes

The furrow is formed by the interface between domains 3a and 3b (Figure 10A). It is part of a long channel spanning the length of Sec1, when connected to the groove in domain 2. SM proteins are largely acidic in the furrow (Misura *et al.,* 2000, Bracher *et al.,* 2000) suggesting that exposed basic patches would be attracted, and acidic patched repelled from this surface. Mapping the yeast Sec1 sequence to the nSec1 structure revealed that Sec1 also has an acidic furrow (Figure 9A).

A random mutagenesis screen performed by Jenna Hutton, Ph.D. resulted in no temperature sensitive mutants mapping to the area of the furrow. An absence of mutants that map to this surface could be explained if either the resulting mutants were not temperature sensitive, or if the mutations in this region were lethal. To explicitly test the furrow as a SNARE complex binding surface, Sec1[G380R,E381K,D429K] was designed to reverse the charges of an acidic patch lining both the top and bottom of the furrow (Figure 9B). As defects in SNARE complex binding correlate with a block in secretion and growth, Sec1 mutants defective in binding are expected to display a temperature sensitive growth defect.

Surprisingly, although the furrow is well conserved, mutant Sec1[G380R,E381K,D429K] demonstrate mild, if any, temperature sensitive growth defect (Figure 5B) and was found to bind SNARE complexes at wild type levels (Figure 4B). Therefore, the evidence from the random and the directed mutants does not support a role for the furrow in SNARE complex binding.

4.4 Sec1 mutants support SNARE complex binding in the lower cleft

The cleft, or central cavity of nSec1, is the binding surface for the closed conformation of a monomeric t-SNARE, syntaxin1a (Misura *et al.,* 2000). Syntaxin1a binds both sides of the 23Å cleft, contacting nSec1 at domains 1 and 3a (Misura *et al*., 2000). While closed syntaxin inhibits the assembly of the SNARE complex, its binding may be important for the organization or subsequent assembly of the other SNAREs (Dulubova *et al.,* 2007). Although Sec1 can not bind monomeric syntaxin (Togneri *et al.,* 2006), it is possible that the syntaxin1a contact site may overlap with the SNARE complex binding surface.

In order to test if the syntaxin1a contact sites on the cleft are important for SNARE complex binding, the syntaxin1a contact site on domain 1 was tested and mutagenized from basic to acidic residues in the Sec1[R63D,K64E] mutant (Figure 9B). Surprisingly, these mutations were lethal. While this result suggests that this location in significant, attempts to isolate a temperature sensitive mutant of this area with mutants Sec1[R63D], Sec1[R63A,K64A], and Sec1[R63A,K64E] all resulted in wild type growth at restrictive

temperature. Therefore, future studies on the significance of the domain 1 patch will require in vitro binding assays with purified Sec1[R63D,K64E] and SNARE complexes.

The syntaxin1a contact site on domain 3a was also examined. A largely acidic patch on the surface of domain 3a was mutagenized to basic residues (Figure 9B). Sec1[E291K,E297R,D360R,D362K] showed no defect in growth at restrictive temperature (Figure 5B) suggesting that the SNARE complex may not share a binding site with syntaxin1a on domain 3a. Alternatively, the SNARE complex may bind residues other than those mutated in Sec1[E291K,E297R,D360R,D362K] which would require future investigation by mutagenesis to probe this region.

In addition to the syntaxin1a contact sites, there is evidence for ligand binding in the lower cleft of Sec1 as demonstrated in a previously studied mutant. Mutant *sec1-31*, or Sec1[F143I,H371R], isolated by Barbara Siminovich-Blok and characterized by Yi-Shan Cheng, demonstrates weaker binding to SNARE complexes at restrictive temperature. This mutant lines both sides of the cleft but is deeply buried. Because we expect to find ligand interaction sites on the surface of proteins, one possibility to explain the binding defect in Sec1[F143I,H371R] is that the mutations indirectly affect SNARE complex binding by altering the protein structures or dynamics.

While there is little evidence to support domain 3a as a SNARE complex binding surface, additional studies may prove the areas in the lower cleft and the top of domain 1 to be

significant. For example, in vitro binding assays of Sec1[R63D,K64E] may be able to provide insight regarding the importance of this region for SNARE complex binding.

4.5 The SNARE complex binding surface includes the groove

The groove describes a 15Å x 15Å x 20Å cavity located between domains 1 and 2 (Figure 10A; Misura *et al.,* 2000). From the nSec1 crystal structure, it is observably the narrowest part of the network of channels that span Sec1 and this groove is seen to continues towards the back of domain 1 (not shown).

Random mutants that map to the groove show diminished binding to the SNARE complex (Yi-Shan Cheng and Jenna Hutton, Ph.D., unpublished observations). Although suggestive, many of these compound mutants have multiple lesions and are buried within the structure. These lesions may therefore contribute indirectly to the SNARE complex binding defect. To test whether the groove is a binding surface for the SNARE complex, site-directed mutagenesis was used to substitute surface exposed basic residues lining the groove with acidic ones in Sec1[K79E,Y80E,R169E,K170E] (Figure 9B).

Sec1[K79E,Y80E,R169E,K170E] was found to have a temperature sensitive growth defect (Figure 5B). To test the binding affinity of Sec1[K79E,Y80E,R169E,K170E], Sec1 was immunoprecipitated and analyzed for coprecipitation with the SNARE complex (Figure 4B). Using this assay, mutations in the groove were found to severely affect

binding of the SNARE complex not only at 38°C, but at 25°C as well, despite the abundance of Sec1 and SNARE complexes (Figure 4B).

Other have proposed that binding in the groove can directly affect syntaxin1a binding in the cleft due to association with opposite sides of the same alpha helix in nSec1 (Misura *et al.,* 2000). The results of our site-directed and random mutagenesis experiments provide strong evidence that the SNARE complex binds the surface of the groove between domains 1 and 2. Binding of the SNARE complex to the groove may, therefore, affect the interaction of Sec1 with another ligand that may be binding the lower cleft. Another possibility is that the SNARE complex binds over a larger surface area, extending from the groove, through the contiguous channel into the lower cleft. Purification and binding analysis of groove mutants are required to examine this possibility. Ultimately, a co-crystal structure of Sec1 and the SNARE complex compared with an uncomplexed Sec1 structure is required to reveal, at atomic resolution, the exact binding interaction and any conformational change that results upon binding of the SNARE complex to Sec1.

Table 1. Viability of Sec1 mutants. Lethal mutants are designated as (∅). Not applicable (N.A.) is used for mutants with wild type growth at 38°C.

Neuronal Residue	Yeast Residue	Restrictive Temperature
D285	D307H	N.A.
H347	H371D	N.A.
D285,H347	D307H,H371D	N.A.
R235,E549	R252E,E604R	∅
R235	R252A	N.A.
E549	E604A	35°C
R235,E549	R252L,E604L	38°C
R235,E549	R252A,E604A	N.A.
D238	D255A	38°C
R235	R252E	38°C
D238	D255N	35°C
R65,E66	R63D,K64E	∅
R65	R63D	N.A.
R65,E66	R63A,K64A	N.A.
R65,E66	R63D,K64E	N.A.
I271,R275,Q336,Q338	E291K,E297R,D360R,D362K	38°C
K356,H357,D403	G380R,E381K,D429K	38°C
E81,K82,E170,R171	K79E,Y80E,R169E,K170E	38°C
R235,D285	R252A,D307H	N.A.
R235,H347	R252A,H371D	35°C
R235,D285,H347	R252A,D307H,H371D	38°C
R235,D238	R252A,D255A	28°C

Table 2. Yeast Strains.

Strain	Genotype	Source
CCY 44	Mat**a** leu2his3ura3metsec1::KANR pR315 *sec1-50* [E604A]	This study
CCY 45	Mat**a** leu2his3ura3metsec1::KANR pR315 *sec1-51* [R252A,D255A]	This study
CCY 46	Mat**a** leu2his3ura3metsec1::KANR pR315 *sec1-52* [D255A]	This study
CCY 48	Mat**a** leu2his3ura3metsec1::KANR pR315 *sec1-63* [R252E]	This study
CCY 51	Mat**a** leu2his3ura3metsec1::KANR pR315 *sec1-66* [R252A, H371D]	This study
CCY 52	Mat**a** leu2his3ura3metsec1::KANR pR315 *sec1-53* [D255N]	This study
CCY 53	Mat**a** leu2his3ura3metsec1::KANR pR315 *sec1-68* [R252A,D307H,H371D]	This study
CCY 54	Mat**a** leu2his3ura3metsec1::KANR pR315 *sec1-54* [R252A,R63A,K64A]	This study
CCY 55	Mat**a** leu2his3ura3metsec1::KANR pR315 *sec1-55* [R252L,E604L]	This study
CCY 64	Mat**a** leu2his3ura3metsec1::KANR pR315 *sec1-56* [R63D]	This study
CCY 65	Mat**a** leu2his3ura3metsec1::KANR pR315 *sec1-57* [R63A,K64A]	This study
CCY 66	Mat**a** leu2his3ura3metsec1::KANR pR315 *sec1-58* [K79E,Y80E,R169E,K170E]	This study
CCY 67	Mat**a** leu2his3ura3metsec1::KANR pR315 *sec1-59* [G380R,E381K,D429K]	This study
CCY 69	Mat**a** leu2his3ura3metsec1::KANR pR315 *sec1-60* [R63A,K64E]	This study
CCY 70	Mat**a** leu2his3ura3metsec1::KANR pR315 *sec1-61* [R252A,E604A]	This study
CCY 86	Mat**a** leu2his3ura3metsec1::KANR pRS416 SEC1	B. Siminovich-Blok
CCY 88	Mat**a** /α his3Δ1/ his3Δ1 leu2/leu2 trp1-289/trp1-289 ura3-52/ ura3-52 pYES/CT SEC1	This study
CCY 89	Mat**a**/α his3Δ1/ his3Δ1 leu2/leu2 trp1-289/trp1-289 ura3-52/ ura3-52 pYES/CT *sec1-61* [R252A,E604A]	This study
CCY 90	Mat**a**/α his3Δ1/ his3Δ1 leu2/leu2 trp1-289/trp1-289 ura3-52/ ura3-52 pYES/CT *sec1-55* [R252L,E604L]	This study
CCY 106	Mat**a** leu2his3ura3metsec1::KANR pR315 *sec1-75* [D307H]	This study
CCY 107	Mat**a** leu2his3ura3metsec1::KANR pR315 *sec1-76* [H371D]	This study
CCY 108	Mat**a** leu2his3ura3metsec1::KANR pR315 *sec1-77* [D307H,H371D]	This study
CCY 109	Mat**a** leu2his3ura3metsec1::KANR pR315 *sec1-78* [R252A]	This study
CCY 110	Mat**a** leu2his3ura3metsec1::KANR pR315 *sec1-79* [E291K,E297R,D360R,D362K]	This study
InvSc1	Mat**a**/α his3Δ1/ his3Δ1 leu2/leu2 trp1-289/trp1-289 ura3-52/ ura3-52 pYES/CT SEC1	Invitrogen

Table 3. Plasmids.

Plasmid	Genotype	Source
pCC 37	pYES/CT SEC1	B. Siminovich-Blok
pCC 64	pRS315 SEC1	B. Siminovich-Blok
pCC 67	pRS315 Sec1 [R252E,E604R]	This study
pCC 72	pRS315 Sec1 [R63D,K64E]	This study
pCC 80	pRS315 Sec1 [R252A,D307H]	This study

Figure 1. Conserved residues and structural properties of SM proteins. A. Highly conserved residues of SM proteins. Residues involved in salt bridges are shown as red spheres, G543 and G544 are shown in blue and D234 and D255 are shown in green. Data collected in phylogeny analysis by Jenna Hutton, Ph.D. B. Conserved salt bridge of domain 2. Shown is the R252-E604 salt bridge and the hydrogen bond acceptor D255. Charges predicted for the side chains at pH 7.4. are shown. C. D255 may fulfill a role as an N-cap by hydrogen bonding to S241. Nitrogen atoms are shown in blue, oxygen atoms are shown in red, hydrogen bond as dashed arrow. Pymol was used to generate the images on the nSec1 structure.

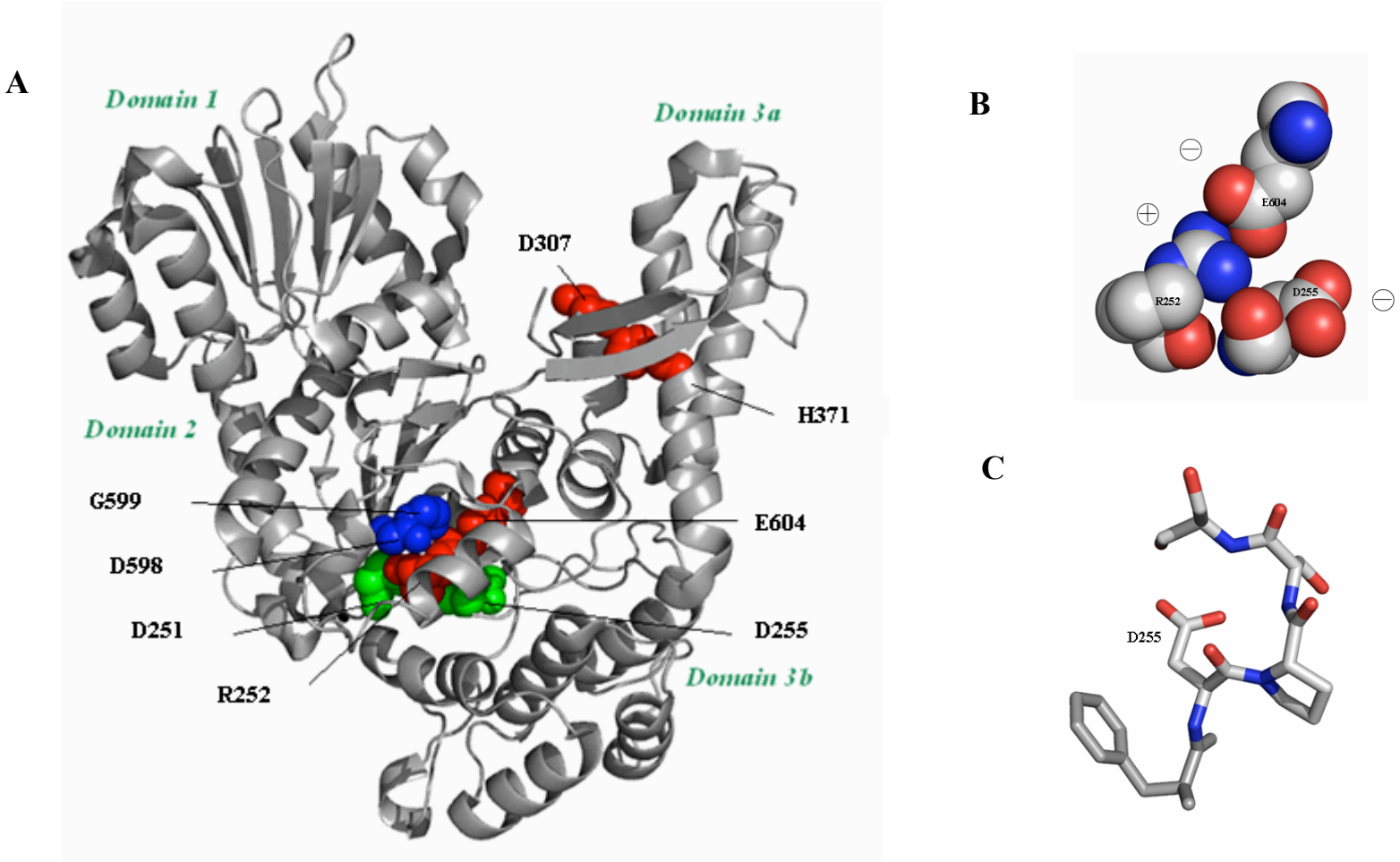

Figure 2. Temperature sensitivity of Sec1 mutants. A. Sec1[E604A] is temperature sensitive at 38°C. Cells were grown to ~0.5OD_{600nm} and resuspended in YPD to 1.0 OD_{600nm} /ml. Cultures were plated in 10-fold serial dilutions starting from 1.0 OD/ml on YPD and incubated at 25°C and 38°C for two days. B. Substitution with hydrophobic residues in Sec1[R252L,E604L] results in a temperature sensitive growth defect. Single colonies were streaked to YPD and incubated at 25°C and 38°C for two days.

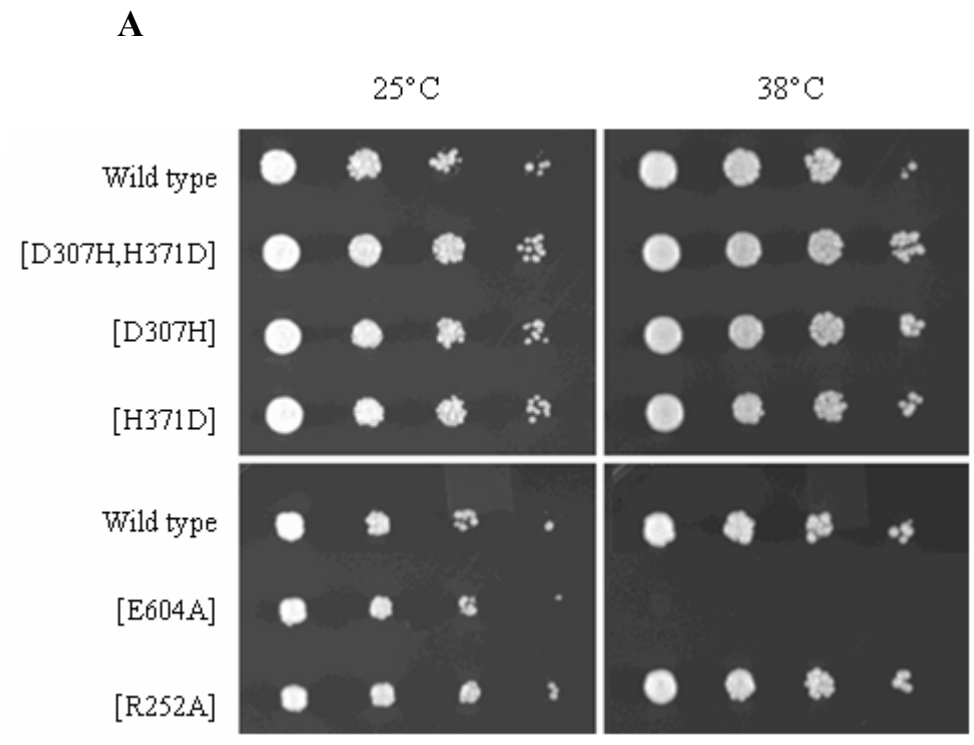

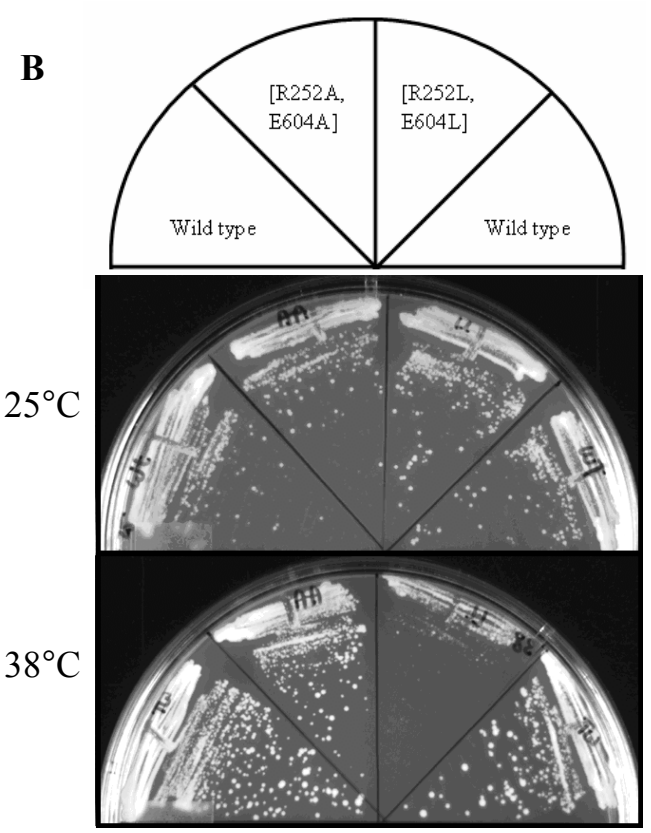

Figure 3. Site-directed mutants of Sec1 are stable and soluble at restrictive temperature. A. Stability of Sec1 protein in wild type and Sec1 mutants. B. Solubility of Sec1 protein in wild type and Sec1 mutants at 13S (13,000 x g), 100S (100,000 x g) and 300S (300,000 x g). Cultures were shifted to restrictive temperature for 20 minutes. WT, wild type.

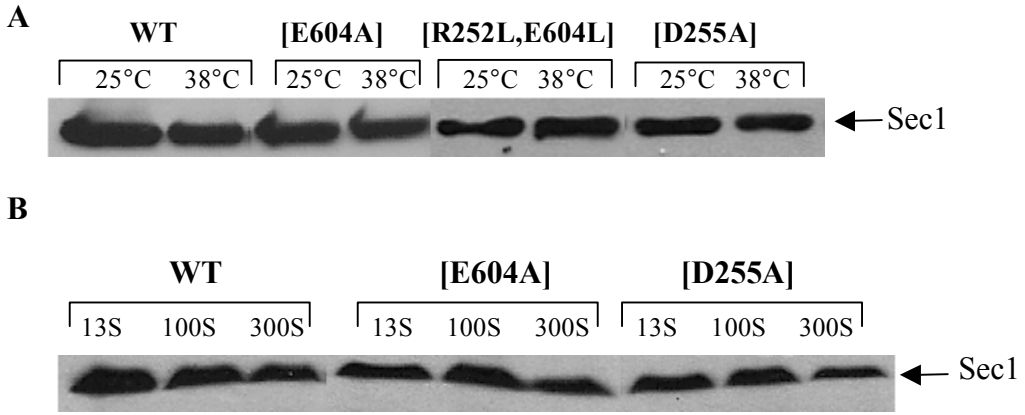

Figure 4. Sec1 mutants show defects in SNARE complex binding. A. Sec1[R252L,E604L] binds fewer SNARE complexes at 38°C and Sec1[R252A,E604A] does not show a binding defect. B. Sec1[K79E,Y80E,R169E,K170E] shows a significant binding defect to SNARE complexes at 25°C and 38°C compared to wild type and Sec1[G380R,E381K,D429K]. The Sec1 IP assays the binding affinity of Sec1 in wild type and mutants for SNARE complexes. Sec9 was immunoprecipitated to measure that abundance of SNARE complexes in wild type and Sec1 mutants. 0.75% of the total lysate is shown (*bottom*). Cells were incubated at 25°C and 38°C for 20 minutes. WT, wild type.

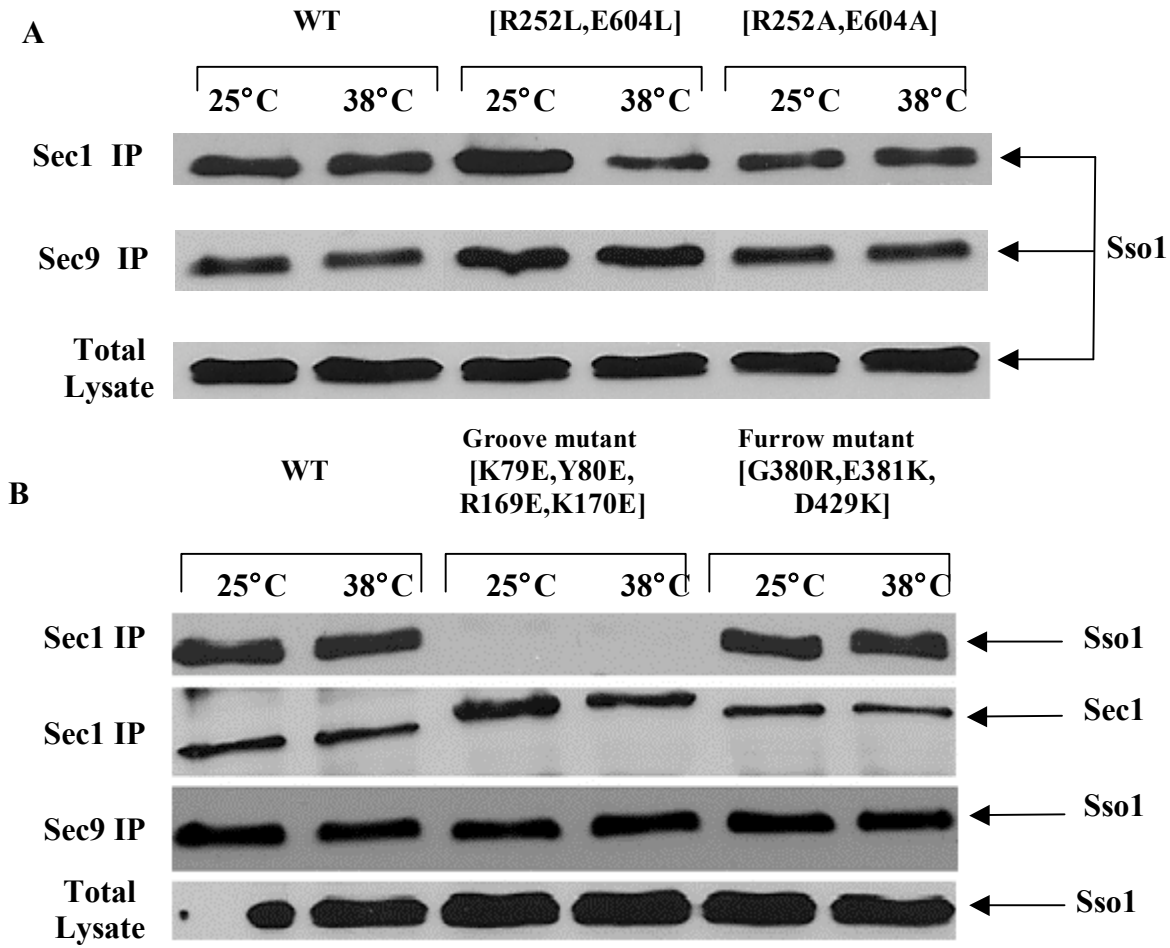

Figure 5. Temperature sensitivity of Sec1 mutants. Sec1[D255A] and Sec1[K79E,Y80E,R169E,K170E] have temperature sensitive growth defects at 38°C. A. One colony was streaked to YPD and incubated at 25°C and 38°C for two days. B. Cells were grown to ~0.5OD_{600nm}, resuspended in YPD to 1.0 OD_{600nm} /ml. Cultures were plated in 10-fold serial dilutions starting from 1.0 OD/ml on YPD and incubated at 25°C and 38°C for two days.

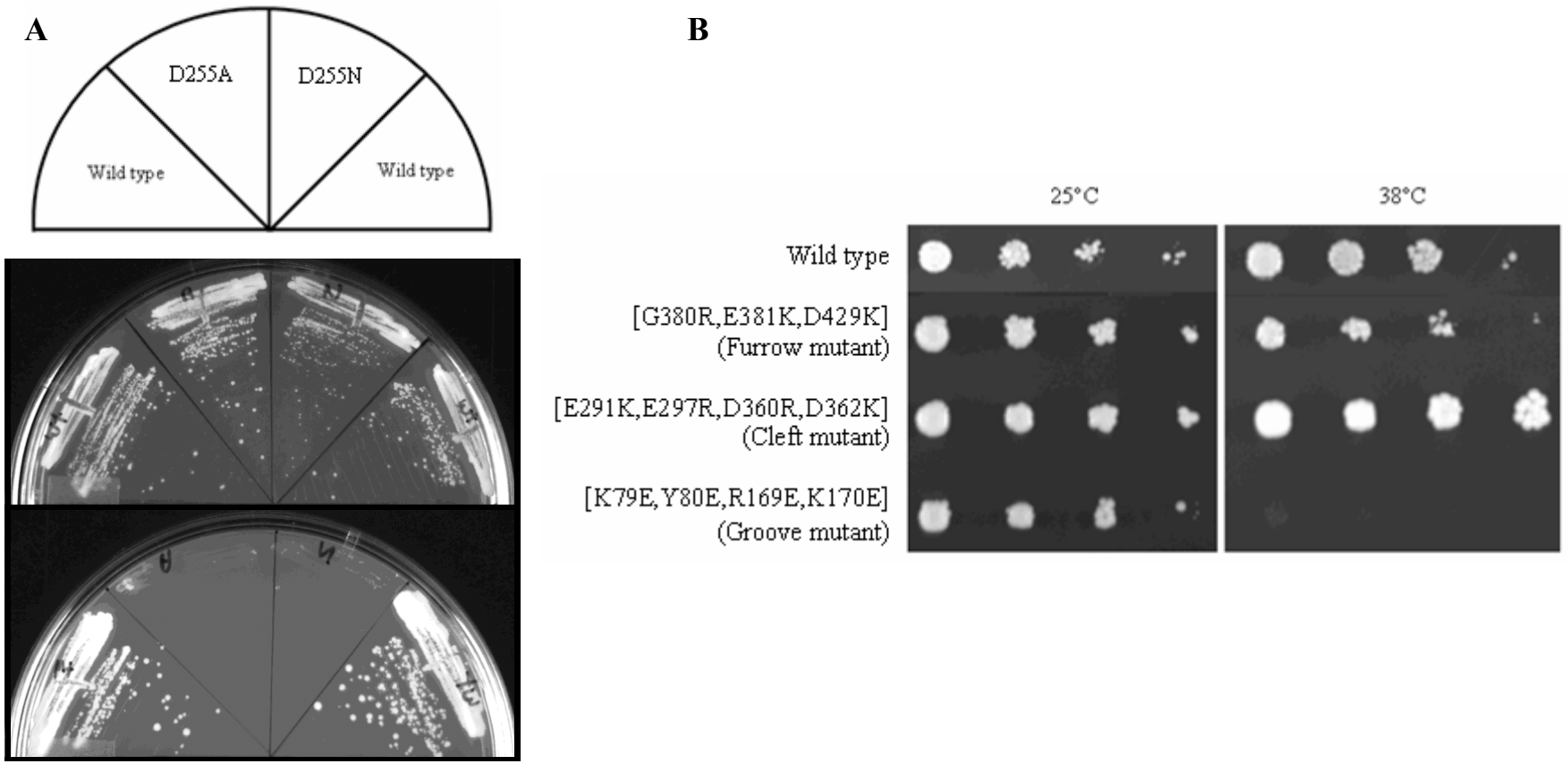

Figure 6. Sec1[E604A] shows diminished binding to the SNARE complex at 38°C and no defect in invertase secretion. A. Sec1 was immunoprecipitated to detect SNARE complex affinity and Sec9 was immunoprecipitated to assay for the total amount of SNARE complexes assembled in the cells. 0.75% of the total lysate is shown (*bottom*). Cells were incubated at 25°C and 38°C for 20 minutes. B.Sec1[E604A] has no defect in invertase secretion. Cells were shifted to 0.1% glucose at 37ºC and an aliquot of cells was removed at different time intervals (maximum 30 minutes) to measure the external and total invertase. See methods. WT, wild type.

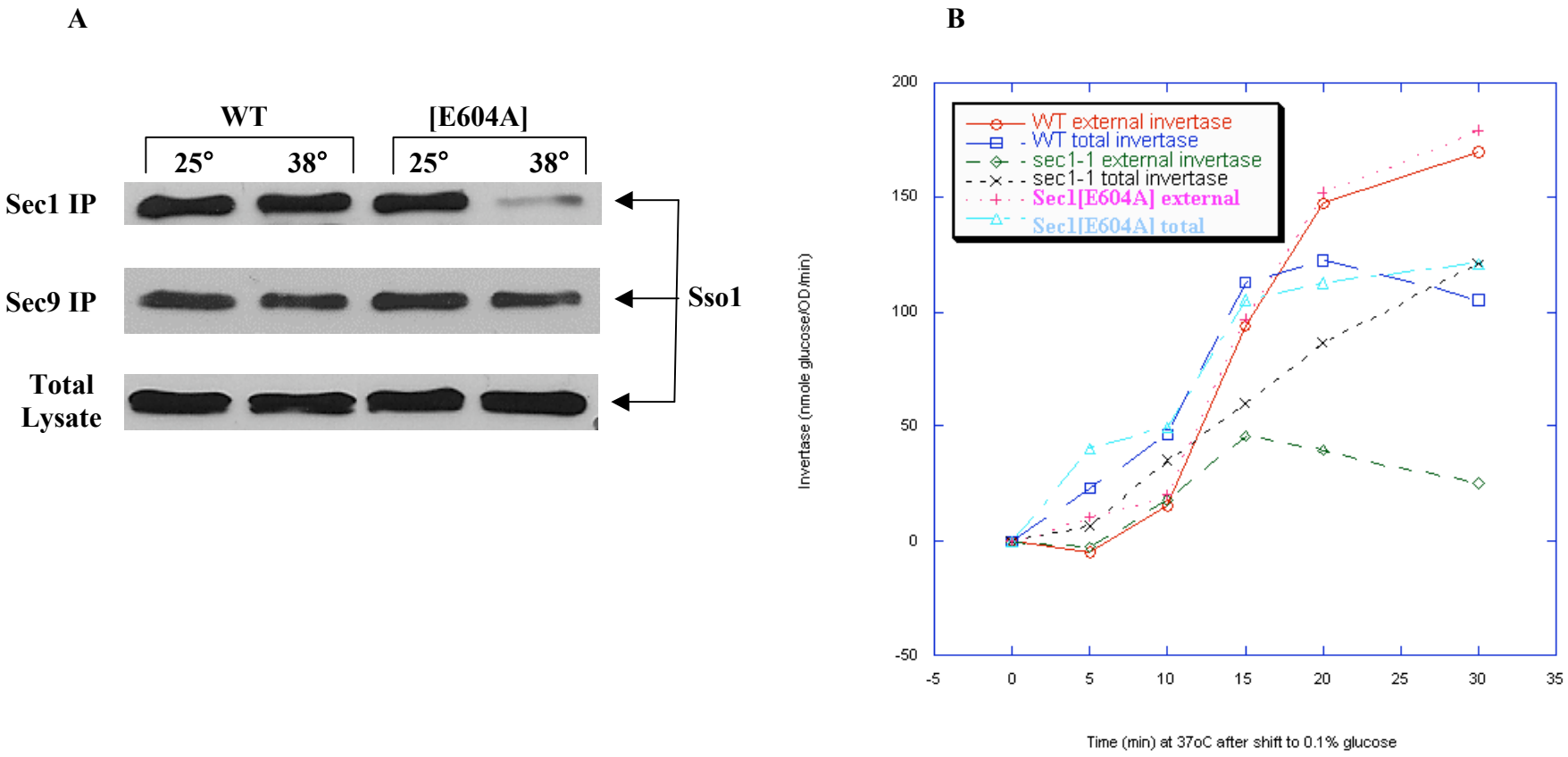

Figure 7. Sec1[E604A] demonstrates a secretion defect by electron microscopy. 100nm vesicles accumulate in Sec1[E604A] at both 25°C and 38°C. Cells were shifted to 38°C for 15 minutes. Bar = 1μm

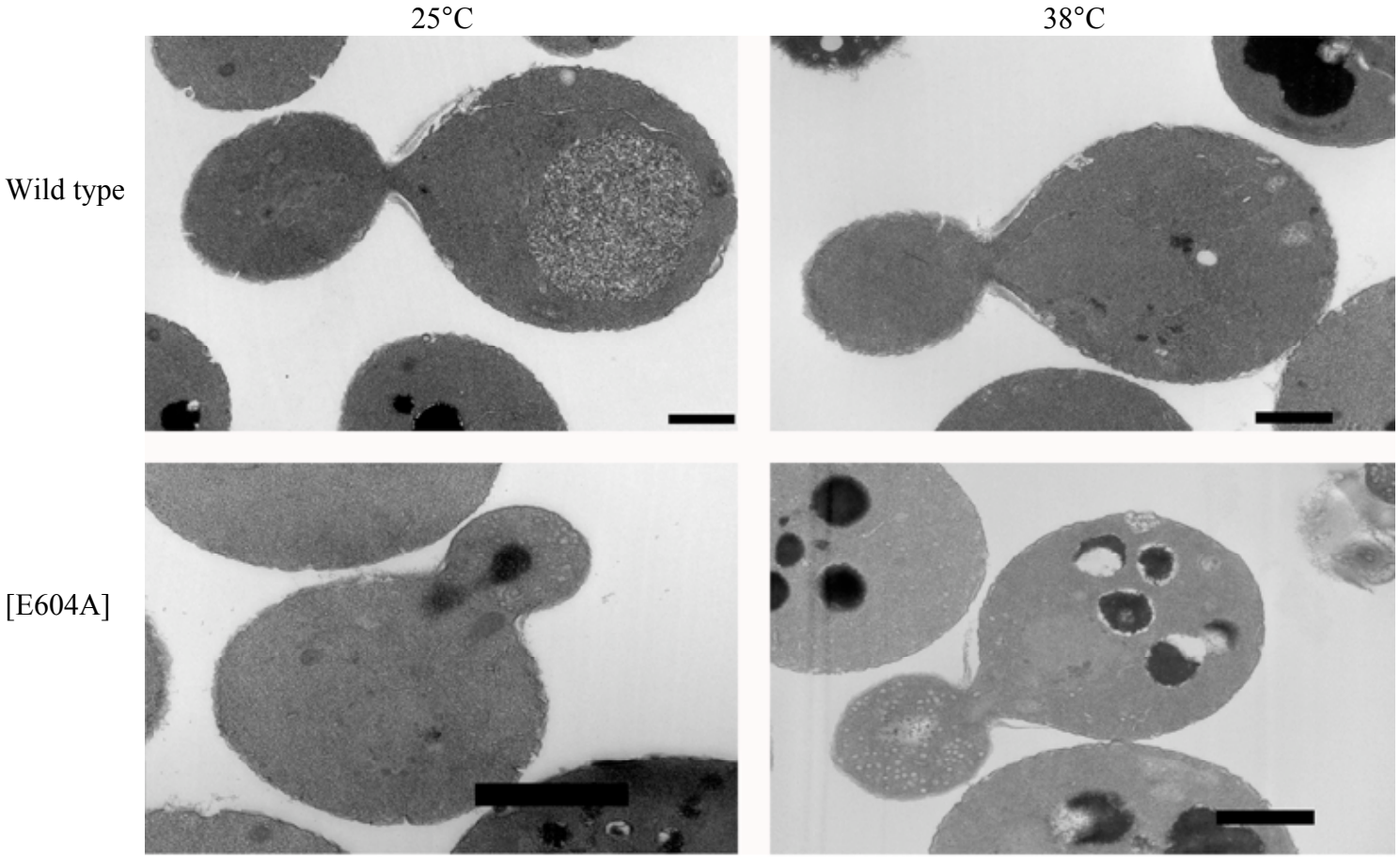

Figure 8. Three classes of Sec1 mutants. Class A mutants have a defect upstream of SNARE complex binding and cluster in domain 2b (shown as orange spheres). Class B mutants are defective in binding to SNARE complexes and cluster in domain 2 (shown as blue spheres). Class C mutants exhibit a temperature sensitive growth defect at 38°C but have no defect in binding to SNARE complexes (shown as green spheres). Random mutants, generated by Jenna Hutton, Ph.D. and assayed by Yi-Shan Cheng, are also shown. Residues were mapped to the structure of neuronal Sec1 (PDB ID# 1DN1) using Pymol. EM, electron microscopy, N.D., Not determined.

Phenotype at restrictive temperature	**Class A**	**Class B**	**Class C**
Stability of Sec1 protein	+	+	+
Abundant SNARE complexes	—	+	+
SNARE complex interaction	—	—	+
Invertase secretion	—	+	N.D.
Polarized vesicle accumulation by EM	+	+	N.D.

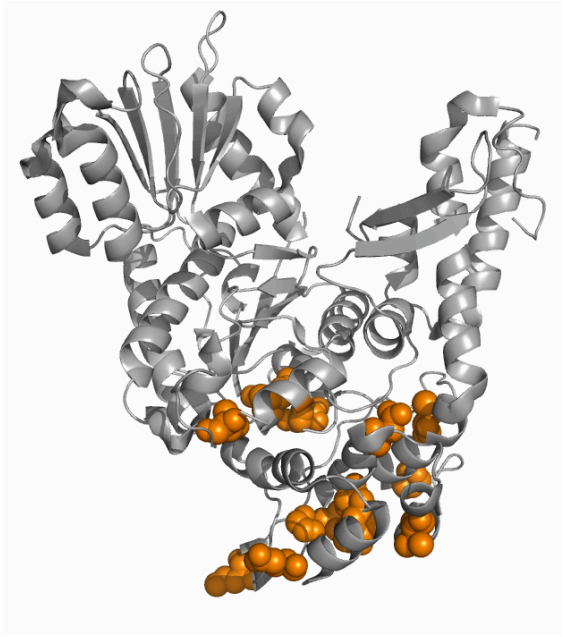

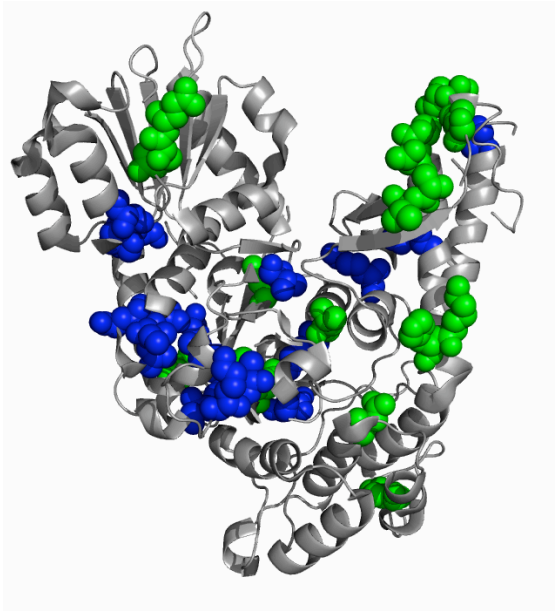

Figure 9. Electrostatic surface potential of yeast Sec1. A. Charged residues in yeast Sec1 mapped to the nSec1 structure. Syntaxin1a has been removed resulting in black spaces. B. Surface patches in yeast were mutagenized to oppositely charged residues compared to wild type (shown in A). Furrow mutant (Sec1[G380R,E381K,D429K] and the Cleft mutant of domain 3a (Sec1[E291K,E297R,D360R,D362K] were mutagenized to basic patches while the Groove mutant (Sec1[K79E,Y80E,R169E,K170E]) and Cleft mutant of domain 1 (Sec1[R63D,K64E]) were mutagenized to acidic patches. Acidic residues are colored in red (Glu, Asp). Basic residues are colored in blue (Lys, Arg, His). Image was generated using Pymol.

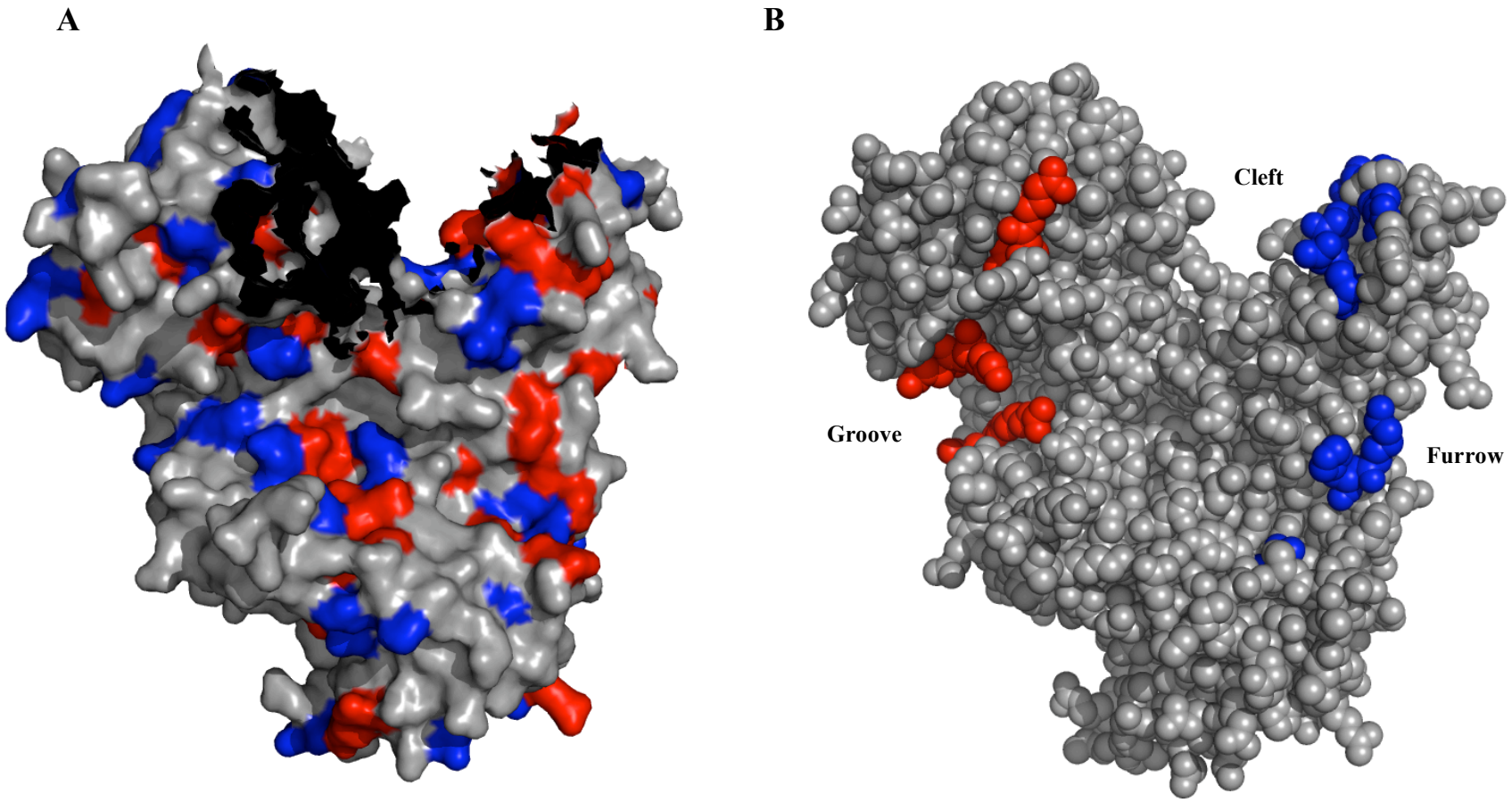

Figure 10. Structural dimensions of nSec1, neuronal and yeast SNARE complexes. A. Measurements of the groove, cleft and furrow in nSec1 structure shown in surface view. Syntaxin1a has been removed resulting in black spaces. B. Crystal structure of the neuronal SNARE complex. C. Crystal structure of the yeast SNARE complex. Dimensions were measured using Pymol.

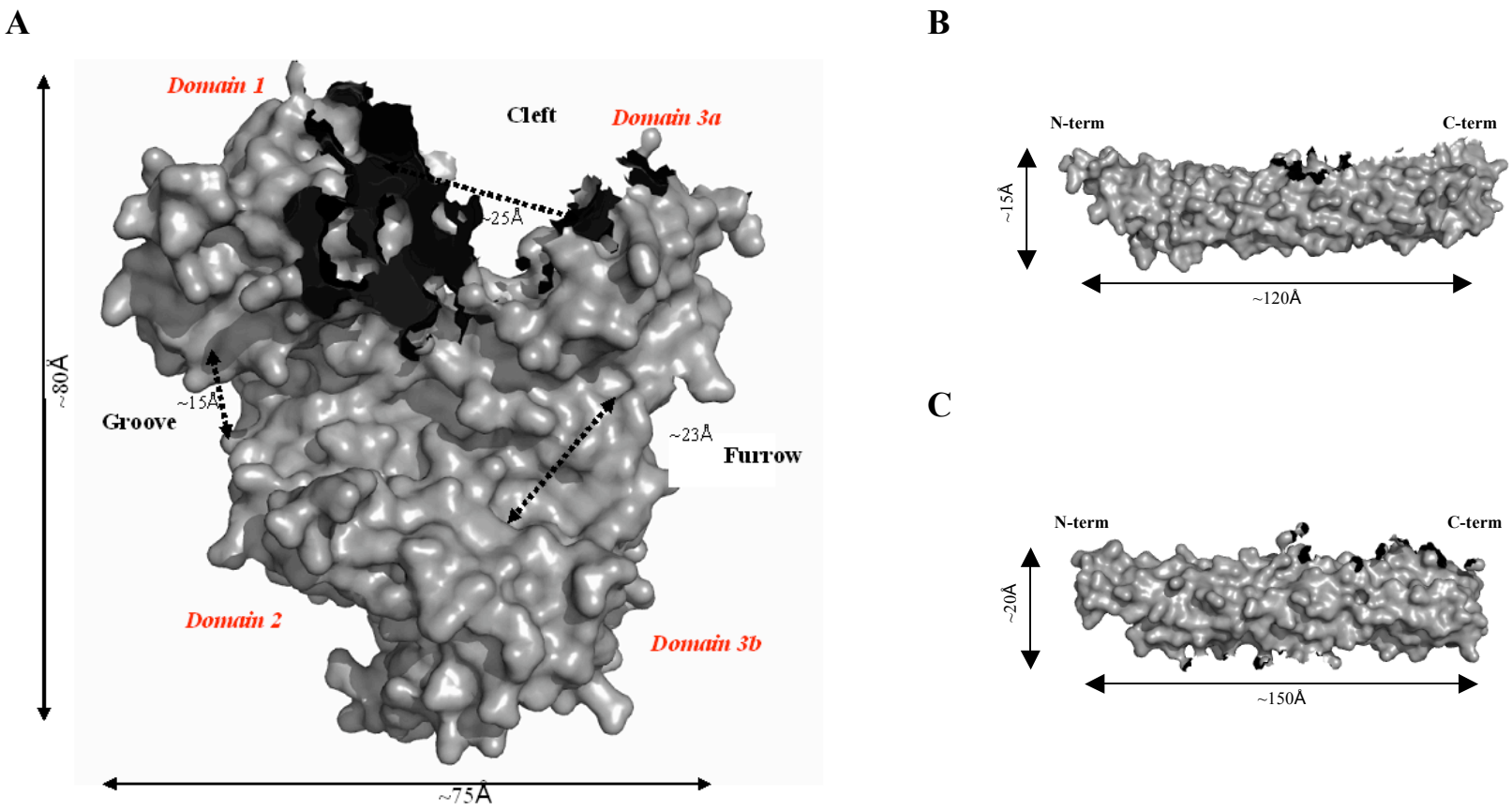

V. Methods and Materials

5.1 Media

Growth media was prepared as described in Guthrie and Fink (1991).

5.2 Strains and Plasmids

Strains and plasmids used and created in this study are listed on Table 2 and 3. Yeast were grown in YPD (2% glucose) broth at 25°C (permissive temperature) or 38°C (restrictive temperature), unless otherwise indicated. Minimal media was used (synthetic complete (SC) lacking indicated amino acids) to grow yeast for stock cultures and for long term storage at -80°C. Bacteria were grown in Luria-Bertani (LB) broth with 50 mg/ml ampicillin (Acros).

5.3 DNA Gel Electrophoresis

DNA was run on 0.8% Ultra-Pure Agarose (Invitrogen) gels in TAE Buffer (0.4M Tris-acetate, 10mM EDTA, pH 8.3) at 100V. The 1 KB ladder molecular weight standard (Invitrogen) was used at 5μg/lane. 10X loading dye was prepared as described in Sambrook *et al*. (2000) and added to the samples.

5.4 Site-directed mutagenesis

5.4.1 Primer Design

Oligonucleotide primers were designed with non-overlapping ends as described in Zheng *et al.* (2004). Briefly, primers were designed to have at least one G or C at the end of each terminus, with a minimum of 8 nonoverlapping bases at the 3' end. Mutations were placed at least 4 bases from the 5' end and at least 6-8 bases from the 3' end. All primers were ordered page-purified from Integrated DNA Technologies, diluted to 50pm/µl in sterile H_2O and stored at -20°C.

5.4.2 PCR

Site-directed mutants were constructed using the Quickchange™ Site-directed Mutagenesis (SDM) Kit II (Stratagene) as directed in the protocol except where otherwise indicated. pRS315SEC1 and pYES/CTSEC1 (Table 2) were used as templates for the PCR reaction. Reactions were in 25µl volumes with an excess of primer as calculated with the equation provided. It should be notes that reagents from the kit are cooperative and can not be substituted. The PCR product was digested with Dpn1 (supplied in the kit) for 3 hours at 37°C. To verify the efficiency of the PCR reaction, 5µl of the final product was run on an agarose gel as described in section 5.3.

5.4.3 E. coli Transformation

The digested DNA was used to transform the competent cells included in the Quickchange kit as described in the manufacturer protocol. Note that no less than 50µl of competent cells should be used for an efficient transformation. Transformed cells were plated to LB/amp and incubated overnight at 37°C or two days at 25°C. For amplification of plasmid DNA, four isolated colonies were picked and inoculated into 2mls of LB with 50mg/ml ampicillin overnight at 37°C. In other cases, electrocompetent DH5α cells were used to transform plasmid DNA as described in Dower *et al.* (1988).

5.4.4 Plasmid Extraction

After amplification in LB/Amp, plasmids were extracted using the Qiagen Plasmid Miniprep Kit as described in the manufacturer protocol.

5.4.5 Restriction Digest

3µl of each pRS315 Sec1 miniprep product was digested with EcoRI (Invitrogen) in a 10µl reaction volume. The reaction was incubated at 37°C for 1 hour and run on a 0.8% agarose gel as described in section 5.3. Digestion of pRS315 Sec1 yields three fragments of ~2.2kb, ~3.5kb and ~4 kb.

pYES/CT Sec1 mutants were double-digested with HindIII (New England Biolabs(NEB)) and XbaI (NEB) in a 10µl reaction volume to release the Sec1 insert yielding two fragments of ~2.4 kb and ~6 kb.

5.4.6 Sequencing

Mutations were confirmed by sequencing in the region of Sec1 DNA. Sequences were viewed using Chromas 2 (www.technelysium.com.au/chromas.html), uploaded into the San Diego Supercomputer (http://seqtool.sdsc.edu) and translated using the SIXFRAME tool. The Basic Local Alignment Search Tool (BLAST) from the National Center for Biotechnology (NCBI) (http://www.ncbi.nlm.nih.gov/blast/Blast.cgi) was used to compare the mutant sequences with wild type Sec1. Once site-directed mutations were confirmed, the whole Sec1 Open Reading Frame (ORF) of temperature sensitive mutants was sequenced to confirm the absence of additional mutations.

5.4.7 Yeast Transformation

Plasmid DNA was transformed into yeast strains CCY 5, for pYES/CT Sec1 mutants, or CCY 86, for pRS315 Sec1 mutants, as described in Gietz *et al.* (2002). pYES/CT Sec1 mutants were plated to minimal media lacking uracil (SC–ura) to select for yeast that have incorporated the URA marked Sec1 plasmid. pRS315 Sec1 mutants were plated to minimal media lacking leucine (SC-leu) then streaked to 5-Fluoroorotic Acid (US Biological), which generates a toxic metabolite in URA+ strains, selecting against the wild type balancer plasmid.

5.4.7 Temperature Sensitivity

Yeast transformants were streaked to YPD plates and incubated for growth at 18°C, 25°C and 38°C to test for cold sensitive or temperature sensitive growth defects. Images were captured using the Quantity One 4.4.1 program and gel-doc (BioRad).

Alternatively, temperature sensitivity of Sec1 mutants was tested using a 48-pin replicator (Boekel). Yeast cultures were grown to linear range, resuspended to 1.0 OD_{600nm}/ ml, diluted in 10-fold serial dilutions and pin-plated to YPD at 18°C, 25°C and 38°C.

5.4.8 Frozen Stocks

Yeast strains were grown for two days at 25°C, suspended in 25% glycerol in minimal media, frozen in liquid nitrogen and stored at -80°C.

5.5 Stability Assay of Sec1

Cells were grown to ~0.5 to1.0 OD_{600nm} and 5 OD_{600nm} units were centrifuged in duplicate at 3,000 rpm for 5 minutes at 25°C. The supernatant was decanted, resuspended and incubated in 1ml of pre-warmed YPD at either 25°C or 38°C for 20 minutes. At the end of the temperature shift, 5 mls of ice-chilled wash buffer (20mM Tris, 20mM Sodium Fluoride, 20mM Sodium Azide) was added and the tubes were set on ice for 5 minutes. The supernatant was completely removed and 100µl of cracking

buffer (8M Urea, 40mM Tris HCl pH 6.8, 0.1mM EDTA, 5% SDS, 0.2mg/ml Bromophenol blue) with 2.5% β-mercaptoethanol (Sigma) was added to each tube, vortexed immediately and boiled for 5 minutes. Cells were centrifuged at 14,000 rpm for 10 minutes to clear cell debris. 0.25 OD_{600nm} of each sample was loaded in a 7.5% polyacrylamide gel for SDS-PAGE and Western blot as described in section 5.8.

5.6 Solubility Assay of Sec1

Cells were grown to ~0.5 to1.0 OD_{600nm} and 40 OD_{600nm} units were resuspended in 5 mls of pre-warmed YPD at 38°C for 20 minutes. 40 mls of ice-chilled wash buffer was added to each tube and set on ice for 5 minutes. Cells were resuspended in 1 ml of chilled lysis buffer (50mM Sodium phosphate pH 7.4, 150 mM Nacl, 1mM EDTA, 0.5% IGEPAL) with added protease inhibitors (10μM antipain, 1μg/ml aprotinin, 30μM leupeptin, 30μM chymostatin, 1μM pepstatin A and 1mM PMSF) and transferred into a chilled tube with 2g of 0.5mm Zirconia/Silica Beads (BioSpec Products). Tubes were centrifuged at 5,000 rpm for 5 minutes at 4°C to pellet cells, additional lysis buffer was added to minimize air space and the cells were lysed in a bead beater for 4 minutes at 4°C. Lysates were sequentially centrifuged at 13,000 x g for 20 minutes (Eppendorf Centrifuge 5417R), 100,000 x g for 30 minutes and 300,000 x g for 30 minutes (Beckman Optima TLX Ultracentrifuge). At the end of each spin, an aliquot of lysate was removed for SDS-PAGE in a 7.5% polyacrylamide gel and Western blot as described in section 5.8.

5.7 Immunoprecipitation (IP)

Cell lysis and immunoprecipitation were performed as described in Carr *et al.* (1999). Briefly, cultures were grown to ~0.5 to1.0 OD_{600nm} and 80 OD_{600nm} units were resuspended in 10ml of YPD pre-warmed to either 25°C or 38°C for 20 minutes. 40 mls of wash buffer was added and the samples were chilled on ice for 5 minutes. Cells were resuspended in 1ml of lysis buffer with added protease inhibitors and transferred to a 2ml chilled screw cap tube with 2g of 0.5mm Zirconia/Silica Beads. Cells were pelleted and the tube was filled with additional lysis buffer to avoid protein denaturation resulting from air in the tubes. A bead beater was used to lyse the cells for 4 minutes at 4°C. The cells were then centrifuged for 15 minutes at 15,000 x g and the lysates were transferred to a new tube. The protein concentration was determined by Bradford Assay (BioRad) using Bovine Serum Albumin as a protein standard. 2mg/ml of lysate was mixed with 50% Protein G-sepharose beads and were left on a shaker for 30 minutes to minimize nonspecific binding of protein to the beads. After centrifugation at 15,000 x g for 30 minutes, 1 ml of cleared lysate was transferred to a new tube in duplicate and incubated with either αSec1 or αSec9 antibody (Covance) for 1 hour. 50% protein G-Sepharose was added to bind the protein-bound antibody and the beads were pelleted and washed four times with lysis buffer lacking protease inhibitors. Proteins were denatured and released from the beads by boiling in Laemmli Solubilizing Buffer (50mM Tris-HCl pH 6.8, 2% SDS, 10% glycerol, BPB) for 5 minutes and then loaded in a 12% polyacrylamide gel for SDS-PAGE and Western blot.

5.8 SDS PAGE/ Western Blot

SDS-PAGE and Western blot were performed as described in Sambrook *et al*. (1989). Precision Plus Protein Standard (BioRad) was used as a molecular weight marker. For detection of Sso1, gels were transferred at 200mA·hrs/gel at a maximum of 200 mA/hour. Sec1 was transferred at 250mA·hrs/gel at 50mA/hour. Rabbit polyclonal antibodies for Sec1 and Sso1 were gifts from Patrick Brennwald, Ph.D. and Mary Munson, Ph.D, respectively.

5.9 Invertase Assay

The invertase assay was performed as described in Schekman *et al.* (1983). Briefly, yeast cultures were grown to ~0.5 to1.0 OD_{600nm} and 7 OD_{600nm} units were resuspended in YPD (2% glucose) for a 1.O OD_{600nm}/ml culture. 1 ml of cells was transferred into a chilled tube containing 10µl 1M Sodium Azide for the zero timepoint, and the remaining cells were resuspended in YP (0.1% glucose) pre-warmed to 38°C to derepress the invertase gene. After 5, 10, 15, 20, and 30 minutes, 1 ml aliquots of cells were transferred into a chilled tube containing 10µl 1M Sodium Azide. Cells were washed three times with 0.5 ml 10mM Sodium Azide and then resuspended in 1 ml of 10mM Sodium Azide. 0.2 ml of this suspension were set aside to measure cell density, 0.4 ml were used to measure total invertase and 0.2 ml for external invertase. For the total invertase, 0.4ml of cells were resuspended in 0.4ml 1% TX-100 (Sigma) to disrupt the plasma membrane and lysed by freeze-thawing for two cycles in liquid nitrogen and a 37°C waterbath.

Levels of total and external invertase were assayed by suspending 5-20µl of cells in 1% TX-100 and 10mM Sodium Azide, for a 20µl total volume, respectively. 25µl of 0.5M Sucrose was added to each tube and the tubes were incubated at 37°C for 30 minutes. 150µl of 0.2M of dibasic Potassium phosphate was added and the tubes were chilled on ice. To liberate the glucose, tubes were boiled for 3 minutes. 1ml of assay mix (500U Glucose Oxidase in 4M Sodium Chloride, 125µg Peroxidase, 7.5mg O-dianisidine, 100µl of 10mM N-ethyl Maleimide, 50ml 0.1M Potassium Phosphate pH 7.0) was added to each tube and the tubes were incubated at 37°C for 30 minutes. 1 ml of 6N Hydrochloric Acid was added to stop the reaction and the amount of glucose was measured against a standard curve of glucose by colorimetric assay.

External levels are greater than total levels of invertase as an outcome of the additional steps in total invertase processing. This assay can be used to characterize mutants as secreting wild type levels of invertase, as mutants that fail to secrete at restrictive temperature and accumulate invertase intracellularly and as mutants that fail to secrete and accumulate (synthesis mutants), as described in Schekman 1983.

5.10 Transmission Electron Microscopy (EM)

Cultures were grown to ~0.5 to1.0 OD_{600nm} and 10 OD_{600nm} units were shifted to restrictive temperature for 10 or 15 minutes. The suspension was vacuum-filtered through a 0.22µ or 0.45µ filter (Corning), washed with 10 mls of 0.1M Cacodylate, pH6.8 (Sigma) and resuspended in 10 mls of 0.1M Cacodylate with 3% Glutaraldehyde

(Electron Microscopy Sciences). The cells were incubated at room temperature for one hour and overnight at 4°C.

The fixed cells were washed twice with 10 ml 50mM Potassium Phosphate, pH 7.5 and resuspended in 2ml Potassium Phosphate with 0.25mg/ml Zymolyase 100T (US Biological) to digest away the cell wall. After incubation for 40 minutes at 37°C with minimal shaking, the cells were washed twice with ice-chilled 0.1M Cacodylate buffer and resuspended in 1 ml of 0.1M Cacodylate buffer. 150µl were placed into each of four tubes, centrifuged to pellet and resuspended in 250µl of ice-chilled 1% Osmium tetroxide. Cells were incubated for 1 hour on ice in the fume hood and then washed three times with 1 ml of sterile H_2O. The supernatant was removed and the cells were incubated in 250µl of 2% Uranyl acetate for 1 hour at room temperature then washed twice with 1 ml of sterile H_2O. After the final wash, the cells were dehydrated using 500µl of 50% then 70% ethanol. Samples were processed by Rajesh Patel at the Electron Microscopy Laboratory at the University of Medicine and Dentistry of New Jersey. Briefly, the cells were further dehydrated in 90% and 100% ethanol followed by acetone. Samples were incubated overnight in Spurr resin, baked at 80°C for 24 hours and 100nm sections were stained with Lead Citrate and Uranyl acetate.

5.11 Differential Interference Contrast (DIC) Microscopy

2 OD_{600nm} cells in log phase were suspended in 100µl YPD and placed on a glass slide for microscopy using a 63X objective lens. To observe yeast at restrictive temperature, cells

were resuspended in 1 ml of pre-warmed YPD at 38°C for 15 minutes. Images were captured using IP Lab (BD Bioscences). A reticule was used to define XY units from pixels to microns.

8.0 Pymol

Pymol and the Pymol user manual were downloaded from the DeLano Scientific website (http://pymol.sourceforge.net) and protein structures from the RCSB Protein Databank (www.rcsb.org). PDB identification numbers of the structures used in this study were 1DN1 (Misura 2000), 1MQS (Bracher 2002), 3B5N (Strop 2008), 1FVF and 1FVH (Bracher 2001) and 1KIL (Chen 2002).

9.0 Alignments

Alignments used in this study were generated by Jenna Hutton, Ph.D. and Chi-Hua Chiu, Ph.D.

Appendix 1

Sec1[R252A,D255A] demonstrates a large cell size compared to wild type

Sec1[R252A,D255A] was designed to test the significance of two conserved residues buried in the core of Sec1. The arginine at 252 is involved in a highly conserved salt bridge and the backbone carbonyl of D255 forms a hydrogen bond with the R252 side chain in the nSec1 structure (Figure 1B). As single substitutions, Sec1[R252A] was not temperature sensitive and Sec1[D255A] exhibited a growth defect only at 38°C (Figure 2, 9). The double mutant of these conserved residues was found to have a temperature sensitive growth defect at 28°C.

To test the binding affinity of Sec1[R252A,D255A] to the SNARE complex, Sec1 was immunoprecipitated and found to coprecipitate with a lower abundance of SNARE complexes than wild type Sec1, suggesting a defect in binding (Appendix Figure A1 C). In addition, in a Sec9 IP, the total abundance of SNARE complexes assembled in Sec1[R252A,D255A] was found to be much lower than in wild type (Appendix Figure A1 C). This mutant showed diminished abundance of SNARE complexes similar to Class A mutants (Table 3). However, unlike the other mutants this class, it was found to have no defect in invertase secretion (Appendix Figure A1 D).

Upon further analysis of Sec1[R252A,D255A], it was discovered that this mutant had an overabundance of Sec1 protein when compared to wild type when standardized by

OD_{600nm} and Bradford Assay (Appendix Figure A1 A,B). Although the mutant was constructed in a centromeric (CEN) vector to minimize copy number, this isolate may have been selected because the excess Sec1 had conferred viability in this otherwise lethal mutant. The larger pool of available Sec1 protein may have compensated for the fewer SNARE complexes available in this mutant leading to a higher likelihood of invertase-containing vesicle fusion. Sec1[R252A,D255A], was also seen to have more abundant levels of Sso1 in the total lysate when compared to wild type (Figure A1C). This is supported by other studies where overexpression of Sec1 was found to increase the levels of SNARE complexes (Wiederkehr 2004).

While phospholipids synthesis continues in *sec* mutants, the plasma membrane no longer expands due to fewer fusion events that add to the plasma membrane (Ramirez *et al.*, 1983). For example, in a *sec1* mutant, while secretion fails at 10-15 minutes after warming to restrictive temperature, a decline in phospholipid synthesis is only seen after 30 minutes or more (Ramirez *et al.*, 1983). The accumulation of intracellular materials in a no-longer expanding membrane leads to increased osmotic sensitivity observed for the mutants at the same time as a secretion defect (Ramirez *et al.*, 1983). This indicates that plasma membrane expansion is directly related to the block in secretion and not as a result of phospholipid biosynthesis (Ramirez *et al.*, 1983).

While Sec1[R252A,D255A] has no block in invertase secretion, there is a clear secretory block in these mutants by EM as vesicles accumulate at 38°C (Appendix Figure A2 C). However, Sec1[R252A,D255A] has a significantly larger cell size when compared to

wild type (Appendix Figure A3). While a round morphology has been reported as a phenotype for some secretory mutants when compared wild type (Wiederkehr 2004), larger cell size is a phenotype not documented for Sec1. It is important to note that overexpression of wild type Sec1 does not lead to larger cell size (Scott *et al.*, 2004, Wiederkehr 2004) ruling out the likelihood that this phenotype was due to increased Sec1 abundance. Upon closer inspection, it was evident that vesicles were accumulating in mostly small and medium budded cells while large budded cells lacked vesicle accumulation by EM (Appendix Figure A2). This phenotype has also been reported for Exo70 and Cdc42 mutants (Adamo *et al.*, 2001 and He *et al.*, 2007), and could suggest a defect at early stages in the cell cycle when growth is highly polarized.

In order to further analyze the phenotype of Sec1[R252A,D255A], future experiments should include an assay for Bgl2 secretion. While a secretory block is visible by EM for these mutants, the lack of an invertase secretion defect suggests a block in a specific subset of secretory vesicles. Assaying for Bgl2 secretion can confirm the specificity of the secretory block and support the similarity of phenotypes between Sec1 mutants and mutants of Exo70 and Cdc42. While Cdc42 is required for actin polarization (Adamo *et al.,* 2001) and Exo70 for targeting vesicles to specific exocytic sites (He *et al.,* 2007), it is possible that Sec1 may be associating with these proteins to coordinate regulation of polarized cell growth. Evidence for any interaction between Sec1 and Exo70 or Cdc42 will require in vitro and in vivo binding studies in the future.

Appendix 2

Mutants of the D307-H371 salt bridge have a temperature sensitive growth defect in a sensitized background

The high conservation of the D307-H371 salt bridge in domain 3a suggests an important role for this salt bridge in SM proteins. In addition, this salt bridge is buried in a region of domain 3 where other known mutants are found to cluster. In the Sec1 homolog, Vps33a, a mutation in domain 3a is found in patients with Hermansky-Pudlak syndrome (Suzuki *et al.*, 2000) and in *Drosophila melanogaster*, mutations in domain 3a of the Sec1 homolog, ROP, leads to loss of function (Wu *et al.*, 1998). Furthermore, domain 3a is an important syntaxin1a contact site in neuronal Sec1 and may be important for defining the perimeter of the cleft between domain 1 and 3a (Figure 8A).

While previous mutants in domain 3a were unable to uncover a temperature sensitive growth defect (see section 2.3), it is possible that the isolated location of this domain (Misura *et al.,* 2000) may have led to the simple compensation of these mutations, with minimal effect on the rest of the Sec1 protein. In an attempt to uncover a temperature sensitive growth defect, the salt bridge mutants were created in the sensitive background of Sec1[R252A]. While R252 is highly conserved, we showed that substitution with alanine does not exhibit a temperature sensitive growth defect (Figure 2A). Furthermore, substitution with glutamic acid at this position results in a temperature sensitive phenotype, but does not affect the function of Sec1[R252E] to bind SNARE complexes

(Appendix Figure A4B). Preliminary studies with double mutants suggested to us that R252A sensitized Sec1 for identification of other mutations, which alone, have no growth defect. We therefore reasoned that the R252A background mutation may provide to be a useful tool for gaining insight into the significance of the D307-H371 salt bridge.

Mutants that were designed (in section 2.4) to destroy or reverse the salt bridge were made in the sensitized R252A background. Although Sec1[R252A, D307H] was not temperature sensitive, Sec1[R252A,H371D] and Sec1[R252A,D307H,H371D] were both found to have temperature sensitive growth defects. Although this could simply be explained by the central and buried location of R252A to be destabilizing, all of the mutants were found to have stable Sec1 at restrictive temperature (Appendix Figure A4 A).

To investigate the effects of the domain 3a salt bridge mutants on Sec1 function, we tested for a SNARE complex binding defect in the sensitized background of R252A. In a Sec1 IP, coprecipitation with the SNARE complex indicated that Sec1[R252A, H371D] was slightly defective in binding SNARE complexes at restrictive temperature (Appendix Figure A4 B). On the other hand, the reversed salt bridge mutant, Sec1[R252A,H371D,D307H], demonstrated a more severe phenotype. In addition to a significant binding defect by Sec1 IP, this mutant showed fewer SNARE complexes after 20 minutes at restrictive temperature (Appendix Figure A4 B), suggesting a secretory lock upstream of SNARE complex assembly.

Figure A1. Sec1[R252A,D255A] has more abundant Sec1, no defect in invertase secretion and a SNARE complex binding defect. A. Sec1 protein in wild type and Sec1[R252A,D255A] strains standardized by OD_{600nm}. B. Sec1 protein in wild type and Sec1[R252A,D255A] strains standardized by protein concentration using Bradford analysis (BioRad). C. Sec1[R252A,D255A] shows fewer SNARE complexes at 38°C by Sec9 IP and diminished binding to SNARE complexes by Sec1 IP. 1% of the total lysate is shown (*bottom*). Cells were incubated at 25°C and 38°C for 20 minutes. D. Sec1[R252A,D255A] has no defect in invertase secretion. Cells were shifted to 0.1% glucose at 37ºC and an aliquot of cells was removed at different time intervals (maximum 30 minutes) to measure the external and total invertase. See methods. WT, wild type.

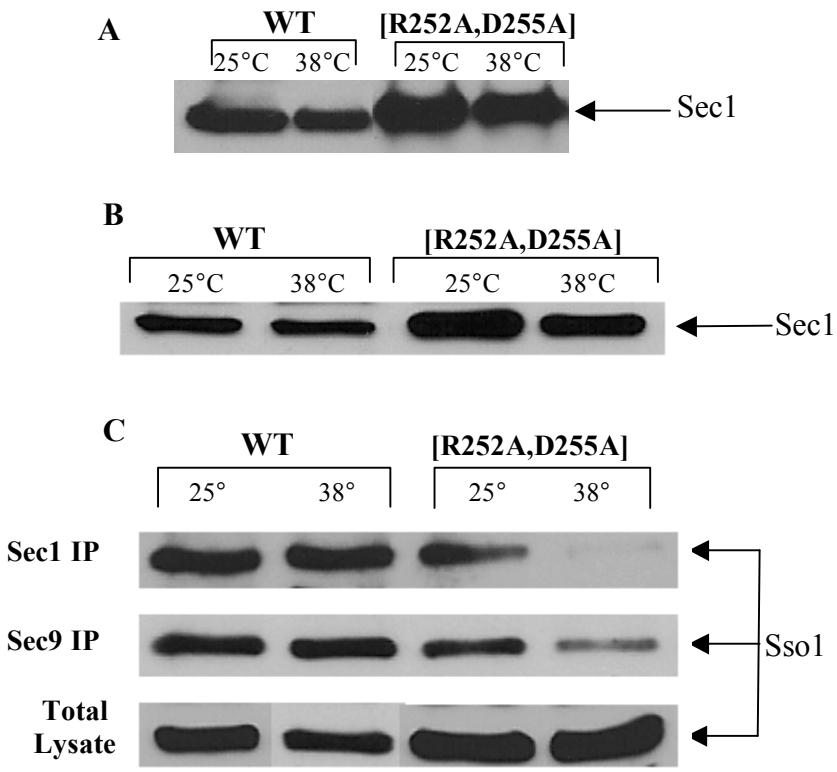

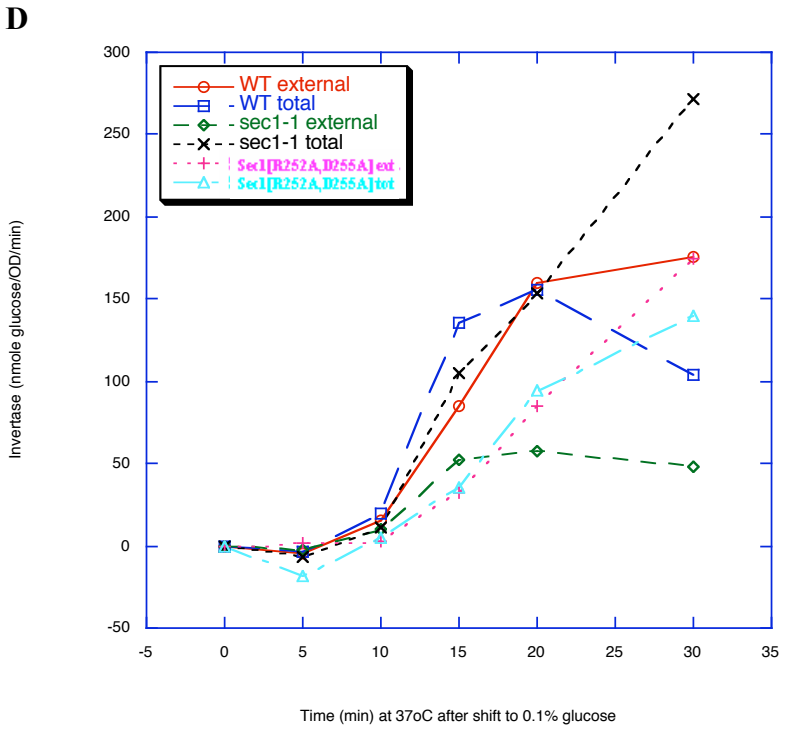

Figure A2. Vesicle accumulation is more evident at early stages of bud growth in Sec1[R252A,D255A]. Electron microscopy was used to compare small and large-budded yeast cells. A, B. Wild type yeast after 15 minutes at 38°C. C, D. Sec1[R252A,D255A] after 10 minutes at 38°C. Bar = 1μm.

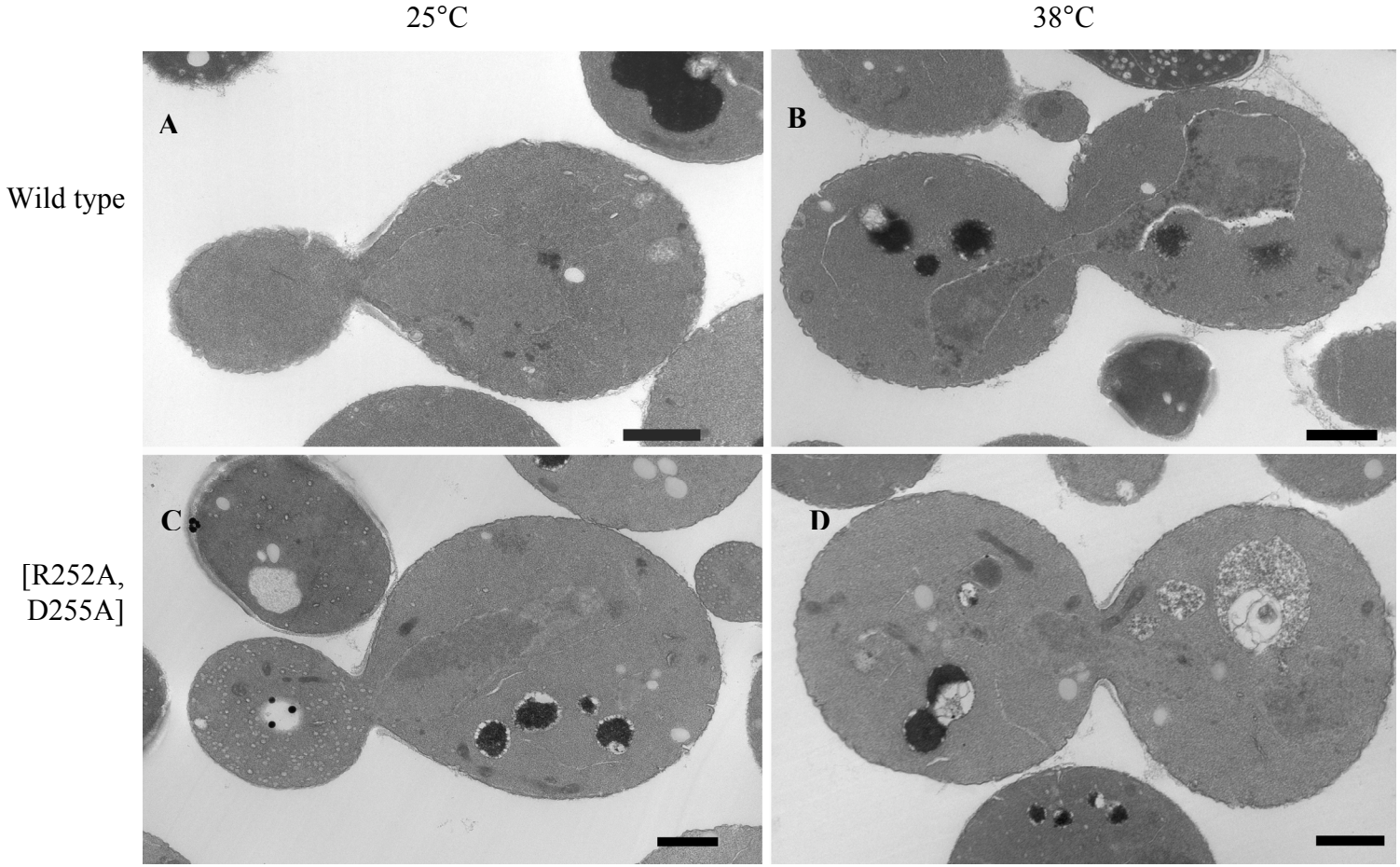

Figure A3. Sec1[R252A,D255A] has a large cell size compared to wild type. A. Wild type yeast at 25°C. B. Wild type yeast at 38° for 15 minutes. C. Sec1[R252A,D255A] at 25°C. D. Sec1[R252A,D255A] at 38°C for 15 minutes. Images were taken using Differential Interference Contrast (DIC) microscopy and 63X objective lens. Bar = 10μm

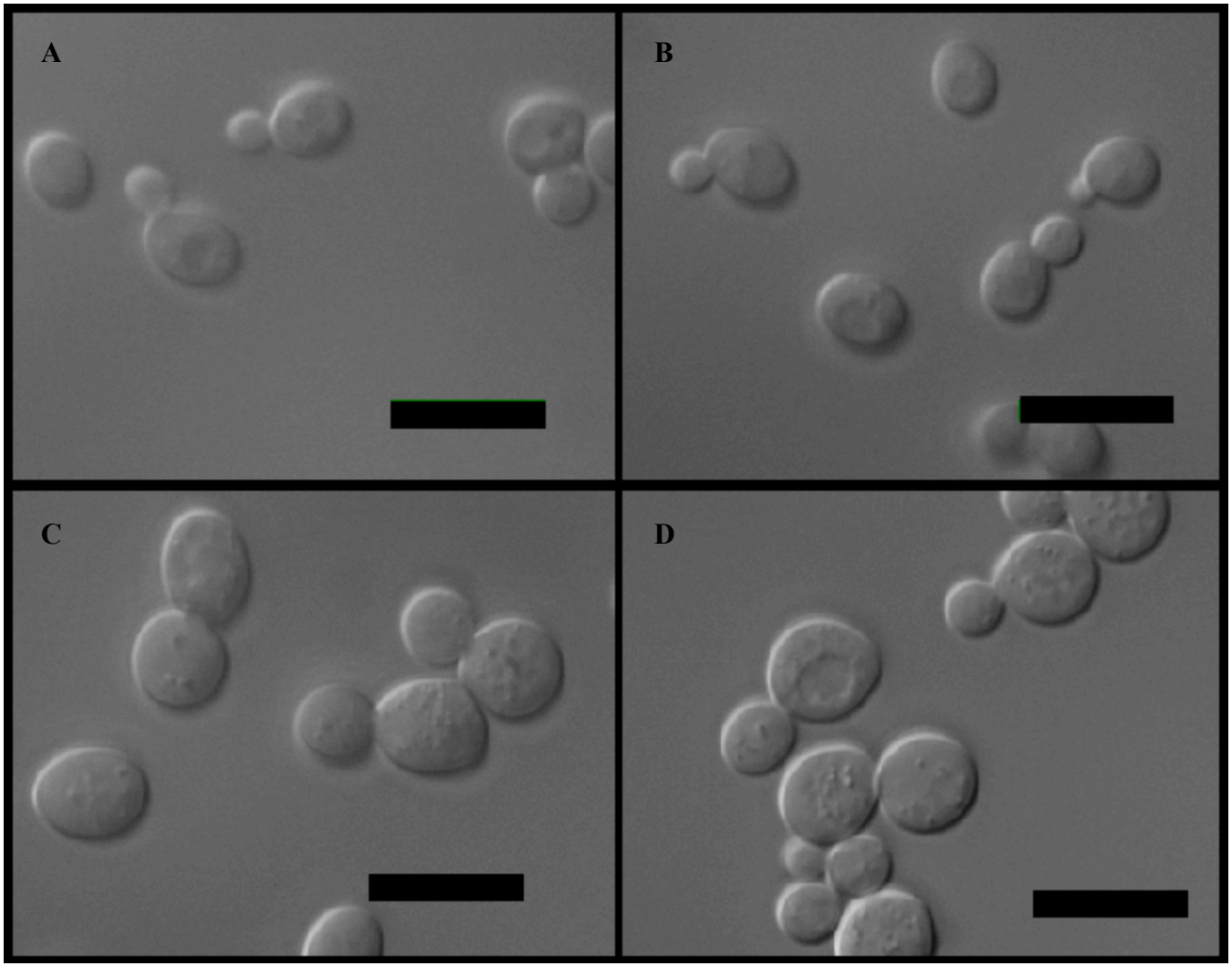

Figure A4. Sec1 mutants of the D307-H371 salt bridge show defects in function. A. Sec1 protein is stable in wild type and mutants at both 25°C and 38°C. B. Using co-immunoprecipitation, Sec1[R252A,H371D] is weakly defective in binding to SNARE complexes by Sec1 IP compared to wild type. Sec1[R252A,D307H,H371D] is defective in binding to SNARE complexes, but also displays fewer SNARE complexes as shown in the Sec9 IP. Sec1[R252E] demonstrates no binding defect. Sec9 IP was not performed on Sec1[R252E]. Cells were incubated for 20 minutes at restrictive temperature.

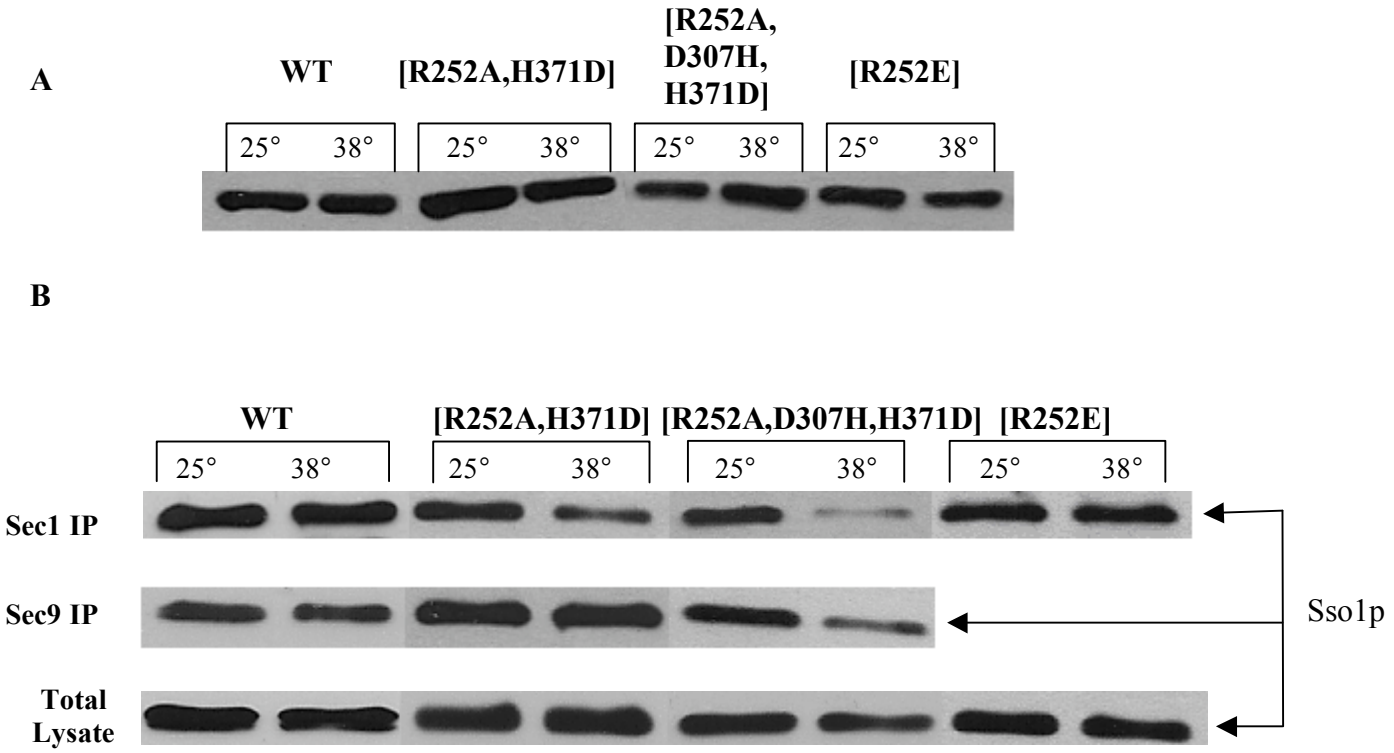

References

Adamo JE, Moskow JJ, Gladfelter AS, Viterbo D, Lew DJ, Brennwald PJ. (2001)Yeast Cdc42 functions at a late step in exocytosis, specifically during polarized growth of the emerging bud. *J Cell Biol.* 2001 Nov 12;155(4):581-92.

Aurora R, Rose GD. (1998) Helix capping. *Protein Sci*. Jan;7(1):21-38.

Banta LM, Vida TA, Herman PK, Emr SD. (1990) Characterization of yeast Vps33p, a protein required for vacuolar protein sorting and vacuole biogenesis. *Mol Cell Biol.* Sep;10(9):4638-49.

Barlow DJ, Thornton JM. (1983) Ion-pairs in proteins. *J Mol Biol*. Aug 25;168(4):867-85.

Boyd C, Hughes T, Pypaert M, Novick P. (2004) Vesicles carry most exocyst subunits to exocytic sites marked by the remaining two subunits, Sec3p and Exo70p. *J Cell Biol.* Dec 6;167(5):889-901.

Bracher A, Perrakis A, Dresbach T, Betz H, Weissenhorn W. (2000) The X-ray crystal structure of neuronal Sec1 from squid sheds new light on the role of this protein in exocytosis. *Structure*. Jul 15;8(7):685-94.

Bracher A, Weissenhorn W. (2001) Crystal structures of neuronal squid Sec1 implicate inter-domain hinge movement in the release of t-SNAREs. *J Mol Biol*. Feb 9;306(1):7-13.

Bracher A, Weissenhorn W. (2002) Structural basis for the Golgi membrane recruitment of Sly1 by Sed5p. *EMBO J.* Nov 15;21(22):6114-24.

Brenner S. (1974) The genetics of Caenorhabditis elegans. *Genetics*. May;77(1):71-94.

Brennwald P, Kearns B, Champion K, Keränen S, Bankaitis V, Novick P. (1994) Sec9 is a SNAP-25-like component of a yeast SNARE complex that may be the effector of Sec4 function in exocytosis. *Cell.* Oct 21;79(2):245-58.

Bryant NJ, James DE. (2003) The Sec1/Munc18 (SM) protein, Vps45p, cycles on and off membranes during vesicle transport. *J Cell Biol.* May 26;161(4):691-6.

Carpp LN, Ciufo LF, Shanks SG, Boyd A, Bryant NJ. (2006) The Sec1/Munc18 protein Vps45p binds its cognate SNARE proteins via two distinct modes. *J Cell Biol.* Jun 19;173(6):927-36.

Carr CM, Chaudhry C, Kim PS. (1997) Influenza hemagglutinin is spring-loaded by a metastable native conformation. *Proc Natl Acad Sci USA*. Dec 23;94(26):14306-13.

Carr CM, Grote E, Munson M, Hughson FM, Novick PJ. (1999) Sec1p binds to SNARE complexes and concentrates at sites of secretion. *J Cell Biol.* Jul 26;146(2):333-44.

Chen X, Tomchick DR, Kovrigin E, Araç D, Machius M, Südhof TC, Rizo J. (2002) Three-dimensional structure of the complexin/SNARE complex. *Neuron*. Jan 31;33(3):397-409.

Cowles CR, Emr SD, Horazdovsky BF. (1994) Mutations in the VPS45 gene, a SEC1 homologue, result in vacuolar protein sorting defects and accumulation of membrane vesicles. *J Cell Sci.* Dec;107 (Pt 12):3449-59.

Doig AJ, Baldwin RL. (1995) N- and C-capping preferences for all 20 amino acids in alpha-helical peptides. *Protein Sci.* Jul;4(7):1325-36.

Dower WJ, Miller JF, Ragsdale CW. (1988) High efficiency transformation of E. coli by high voltage electroporation. *Nucleic Acids Res.* Jul 11;16(13):6127-45.

Dulubova I, Khvotchev M, Liu S, Huryeva I, Südhof TC, Rizo J. (2007) Munc18-1 binds directly to the neuronal SNARE complex. *Proc Natl Acad Sci USA.* Feb 20;104(8):2697-702.

Dulubova I, Yamaguchi T, Gao Y, Min SW, Huryeva I, Südhof TC, Rizo J. (2002) How Tlg2p/syntaxin 16 'snares' Vps45. *EMBO J*. Jul 15;21(14):3620-31.

Fasshauer D, Sutton RB, Brunger AT, Jahn R. (1998) Conserved structural features of the synaptic fusion complex: SNARE proteins reclassified as Q- and R-SNAREs. *Proc Natl Acad Sci USA*. Dec 22;95(26):15781-6.

Fontana A, de Laureto PP, Spolaore B, Frare E, Picotti P, Zambonin M. (2004) Probing protein structure by limited proteolysis. *Acta Biochim Pol.* 51(2):299-321.

Gietz RD, Schiestl RH. (2007) Quick and easy yeast transformation using the LiAc/SS carrier DNA/PEG method. *Nat Protoc.* 2(1):35-7.

Grabowski R, Gallwitz D. (1997) High-affinity binding of the yeast cis-Golgi t-SNARE, Sed5p, to wild-type and mutant Sly1p, a modulator of transport vesicle docking. *FE BS Lett*. Jul 14;411(2-3):169-72.

Grote E, Carr CM, Novick PJ. (2000) Ordering the final events in yeast exocytosis. *J Cell Biol.* Oct 16;151(2):439-52.

Guo W, Grant A, Novick P. (1999) Exo84p is an exocyst protein essential for secretion. *J Biol Chem.* Aug 13;274(33):23558-64.

Guthrie C, Fink GR. (1991) *Guide to Yeast Genetics and Molecular Biology. Methods in Enzymology* Vol 94. San Diego, CA: Academic Press

Harsay E, Bretscher A. (1995) Parallel secretory pathways to the cell surface in yeast. *J Cell Biol.* Oct;131(2):297-310.

He B, Xi F, Zhang J, TerBush D, Zhang X, Guo W. (2007) Exo70p mediates the secretion of specific exocytic vesicles at early stages of the cell cycle for polarized cell growth. *J Cell Biol.* Mar 12;176(6):771-7.

Hendsch ZS, Tidor B. (1994) Do salt bridges stabilize proteins? A continuum electrostatic analysis. *Protein Sci.* Feb;3(2):211-26.

Hu C, Hardee D, Minnear F. (2007) Membrane fusion by VAMP3 and plasma membrane t-SNAREs. *Exp Cell Res*. Sep 10;313(15):3198-209.

Hutton JL, Chiu C, Carr C. Conserved amino acids distinguish Sec1, Sly1p, Vps33, Vps45 for selective vesicle membrane fusion. In review.

Jeffrey PD, Bewley MC, MacGillivray RT, Mason AB, Woodworth RC, Baker EN. (1998) Ligand-induced conformational change in transferrins: crystal structure of the open form of the N-terminal half-molecule of human transferrin. *Biochemistry*. Oct 6;37(40):13978-86.

Koenderink JB, Swarts HG, Willems PH, Krieger E, De Pont JJ. (2004) A conformation-specific interhelical salt bridge in the K+ binding site of gastric H,K-ATPase. *J Biol Chem*. Apr 16;279(16):16417-24.

Kumar S, Nussinov R. (1999) Salt bridge stability in monomeric proteins. *J Mol Biol.* Nov 12;293(5):1241-55.

Li Y, Gallwitz D, Peng R. (2005) Structure-based functional analysis reveals a role for the SM protein Sly1p in retrograde transport to the endoplasmic reticulum. *Mol Biol Cell.* Sep;16(9):3951-62.

Misura KM, Scheller RH, Weis WI. (2000) Three-dimensional structure of the neuronal-Sec1-syntaxin 1a complex. *Nature*. Mar 23;404(6776):355-62.

Novick P, Schekman R. (1979) Secretion and cell-surface growth are blocked in a temperature-sensitive mutant of Saccharomyces cerevisiae. *Proc Natl Acad Sci USA*. Apr;76(4):1858-62.

Olkkonen VM, Ikonen E. (2000) Genetic defects of intracellular-membrane transport. *N Engl J Med.* Oct 12;343(15):1095-104.

Ossig R, Dascher C, Trepte HH, Schmitt HD, Gallwitz D. (1991) The yeast SLY gene products, suppressors of defects in the essential GTP-binding Ypt1 protein, may act in endoplasmic reticulum-to-Golgi transport. *Mol Cell Biol*. Jun;11(6):2980-93.

Peng R, Gallwitz D. (2004) Multiple SNARE interactions of an SM protein: Sed5p/Sly1p binding is dispensable for transport. *EMBO J.* Oct 13;23(20):3939-49.

Pfeffer SR. (1999) Transport-vesicle targeting: tethers before SNAREs. *Nat Cell Biol.* May;1(1):E17-22.

Rajavel M, Gross J, Segura E, Moore WT, Grubmeyer C. (1996) Limited proteolysis of Salmonella typhimurium nicotinic acid phosphoribosyltransferase reveals ATP-linked conformational change. *Biochemistry*. Apr 2;35(13):3909-16.

Ramirez RM, Ishida-Schick T, Krilowicz BL, Leish BA, Atkinson KD. (1983). Plasma membrane expansion terminates in *Saccharomyces cerevisiae* Secretion-defective mutants while phospholipids synthesis continues. *J of Bact.* Jun:154(3): 1276-1283

Sambrook J, Fritsch EF, Maniatis T. (1989) *Molecular Cloning: A Laboratory Manual* (2nd Ed.). Cold Spring Harbor, NY: Cold Spring Harbor Laboratory Press

Schekman R, Esmon B, Ferro-Novick S, Field C, Novick P. (1983) Yeast secretory mutants: isolation and characterization. *Methods Enzymol.* 96:802-15.

Schueler O, Margalit H. (1995) Conservation of salt bridges in protein families. *J Mol Biol.* Apr 21;248(1):125-35.

Scott BL, Van Komen JS, Irshad H, Liu S, Wilson KA, McNew JA. (2004) Sec1p directly stimulates SNARE-mediated membrane fusion in vitro. *J Cell Biol.* Oct 11;167(1):75-85.

Shen J, Tareste DC, Paumet F, Rothman JE, Melia TJ. (2007) Selective activation of cognate SNAREpins by Sec1/Munc18 proteins. *Cell*. Jan 12;128(1):183-95.

Stockner T, Vogel HJ, Tieleman DP. (2005) A salt-bridge motif involved in ligand binding and large-scale domain motions of the maltose-binding protein. *Biophys J*. Nov;89(5):3362-71.

Strop P, Kaiser SE, Vrljic M, Brunger AT. (2008) The structure of the yeast plasma membrane SNARE complex reveals destabilizing water-filled cavities. *J Biol Chem*. Jan 11;283(2):1113-9.

Sutton RB, Fasshauer D, Jahn R, Brunger AT. (1998) Crystal structure of a SNARE complex involved in synaptic exocytosis at 2.4 A resolution. *Nature*. Sep 24;395(6700):347-53.

Suzuki T, Oiso N, Gautam R, Novak EK, Panthier JJ, Suprabha PG, Vida T, Swank RT, Spritz RA. (2000) The mouse organellar biogenesis mutant buff results from a mutation

in Vps33a, a homologue of yeast vps33 and Drosophila carnation. *Proc Natl Acad Sci USA*. Feb 4;100(3):1146-50.

TerBush DR, Maurice T, Roth D, Novick P. (1996) The Exocyst is a multiprotein complex required for exocytosis in Saccharomyces cerevisiae. *EMBO J.* Dec 2;15(23):6483-94.

Tissot AC, Vuilleumier S, Fersht AR. (1996) Importance of two buried salt bridges in the stability and folding pathway of barnase. *Biochemistry*. May 28;35(21):6786-94.

Togneri J, Cheng YS, Munson M, Hughson FM, Carr CM. (2006) Specific SNARE complex binding mode of the Sec1/Munc-18 protein, Sec1p. *Proc Natl Acad Sci USA*. 2006 Nov 21;103(47):17730-5.

Toonen RF, Verhage M. (2003) Vesicle trafficking: pleasure and pain from SM genes. *Trends Cell Biol.* Apr;13(4):177-86.

Walworth NC, Novick PJ. (1987) Purification and characterization of constitutive secretory vesicles from yeast. *J Cell Biol.* Jul;105(1):163-74.

Weber T, Zemelman BV, McNew JA, Westermann B, Gmachl M, Parlati F, Söllner TH, Rothman JE. (1998) SNAREpins: minimal machinery for membrane fusion. *Cell*. Mar 20;92(6):759-72.

Wiederkehr A, De Craene JO, Ferro-Novick S, Novick P. (2004) Functional specialization within a vesicle tethering complex: bypass of a subset of exocyst deletion mutants by Sec1p or Sec4p. *J Cell Biol.* Dec 6;167(5):875-87.

Wu MN, Littleton JT, Bhat MA, Prokop A, Bellen HJ. (1998) ROP, the Drosophila Sec1 homolog, interacts with syntaxin and regulates neurotransmitter release in a dosage-dependent manner. *EMBO J*. Jan 2;17(1):127-39.

Zhou HX, Lyu P, Wemmer DE, Kallenbach NR. (1994) Alpha helix capping in synthetic model peptides by reciprocal side chain-main chain interactions: evidence for an N terminal "capping box". *Proteins*. Jan;18(1):1-7.